MATHEMATICS OF COMPUTATION
Volume 00, Number 0, Pages 000–000
S 0025-5718(XX)0000-0

APPLICATION OF GENERALIZED GAUSS–RADAU PROJECTIONS FOR THE LOCAL DISCONTINUOUS GALERKIN METHOD FOR LINEAR CONVECTION-DIFFUSION EQUATIONS

YAO CHENG, XIONG MENG, AND QIANG ZHANG

Abstract. In this paper we consider the local discontinuous Galerkin method based on the generalized alternating numerical fluxes, for solving the linear convection-diffusion equations in one dimension and two dimensions. As an application of generalized Gauss–Radau projections, we get rid of the dual argument and obtain directly the optimal L^2-norm error estimate in a uniform framework. The sharpness of the theoretical results is demonstrated by numerical experiments.

1. Introduction

In this paper we continue the work [20] and apply the generalized Gauss–Radau projection to study the local discontinuous Galerkin (LDG) method based on generalized alternating numerical fluxes (see, for example, (2.8) and (2.16) below) to solve linear convection-diffusion problem

$$\frac{\partial u}{\partial t}+\sum_{\ell=1}^{m}\frac{\partial}{\partial x_\ell}\Big(c_\ell u\Big)-\sum_{\ell=1}^{m}\frac{\partial}{\partial x_\ell}\Big(d_\ell\frac{\partial u}{\partial x_\ell}\Big)=f(x_1,\dots,x_m,t),\quad m=1,2, \tag{1.1}$$

in domain $\Omega=(0,2\pi)^m\subset\mathbb{R}^m$ for any time $t\in(0,T]$, where c_ℓ, $d_\ell\geq 0$, and f are the given functions. Here the generalized alternating numerical flux is used to distinguish with the purely alternating numerical flux. From the view of practice, the generalized alternating numerical flux is used more widely, since the purely alternating numerical flux is not easy to define for linear equations with varying-coefficient, or even nonlinear equations. For simplicity, we assume that c_ℓ and d_ℓ are constants, and mainly consider the periodic boundary condition in this paper.

Received by the editor June 6, 2015 and, in revised form, October 28, 2015.

2010 *Mathematics Subject Classification.* Primary 65M12, 65M15, 65M60.

Key words and phrases. local discontinuous Galerkin method, convection-diffusion equation, error estimates, generalized Gauss–Radau projection.

The research of the first author was supported by NSFC grant 11271187 and the program B for outstanding PhD candidate of Nanjing University.

The research of the second author was supported by PIRS of HIT grant B201404, and NSFC grant 11501149. Additional support was provided by the EU under the 7th Framework Programme Marie Curie International Incoming Fellowships FP7-PEOPLE-2013-IIF, GA number 622845 while the author was in residence at University of East Anglia, United Kingdom.

The research of the third author was supported by NSFC grant 11271187.

The LDG method to solve (1.1) has been introduced firstly by Cockburn and Shu [13], which is motivated by the work of Bassi and Rebay [1] for computing Navier–Stokes problems. As a special class of discontinuous Galerkin (DG) method, the main technique of the LDG method is to rewrite (1.1) into an equivalent system containing only first-order derivatives, which can further be discretized by the standard DG method [21, 11]. An important ingredient in the design of the LDG method is the choice of numerical flux, which should ensure the stability and high order accuracy feature of the scheme. Since discontinuous finite element spaces do not require any continuity at interface boundaries, the method has enough flexibility to deal with complex domain and adaptive computation. For a fairly complete set of references about the method and its implementation, please refer to the review papers [14, 23] and recent books [3, 15, 18].

The a priori estimate of the LDG method to solve (1.1) has been studied for a long period, in which different numerical fluxes are considered. From the point of view of numerical experiments, this method often displays the optimal error estimate in the L^2-norm. However, it is rather difficult to derive optimal convergence results theoretically for general cases, with difficulties arising from different choice of numerical fluxes and different triangulations. To express this clearly, let us recall some important results available in the current literature for the linear convection-diffusion problems on the Cartesian mesh. In [13], the authors have considered the generalized alternating numerical fluxes, and only obtained the suboptimal error estimate of order k in the L^2-norm by virtue of the local L^2-projection. Here and in what follows, k is the degree of piecewise polynomials in the discontinuous finite element space. The optimal convergence results of order $k+1$ is lost because the projection error at all element boundaries cannot be treated in a nice way. In light of this point, the optimal error estimate is obtained [4] for the special case in which the purely alternating numerical flux is used, by using the definition and approximation properties of the so-called local Gauss–Radau projections. Thanks to exact collocation of the local Gauss–Radau projections at one of end points of each element in one-dimensional case, the projection error at element boundary is successfully eliminated. Similar results for two-dimensional case can also be established by observing the super-convergence property of DG discretization on each element. However, when the generalized, not purely, alternating numerical fluxes are used, the local Gauss–Radau projection does not work well. Hence, to obtain the optimal error estimate, we have to construct and analyze some suitable projections.

It is therefore important and interesting to fill up the above gap by establishing the optimal convergence results of the LDG method with generalized numerical fluxes for convection-diffusion equations. This paper is the continued work of Meng, Shu and Wu [20], in which optimal error estimates are obtained for the DG method based on upwind-biased numerical fluxes for linear hyperbolic problems, in one- and two-dimensional Cartesian meshes. The main technical difficulty is the construction and analysis of some suitable projections tailored to the very choice of the numerical fluxes. Instead of the standard local Gauss–Radau projections, the resulting projections in [20] and in the current paper are globally coupled, which will definitely increase the difficulty in the analysis of the newly designed *generalized Gauss–Radau projections*, even for the existence of the projections. The idea of

constructing such global projections is motivated by earlier work of Cheng and Shu in [7], and the recent work of Bona et al. [2] for solving generalized KdV equations.

The objective of this paper is to take advantage of the generalized Gauss–Radau projections, and to derive the optimal error estimate in the L^2-norm for the LDG method with generalized alternating fluxes. To be specific, we want to prove the $(k+1)$-th order convergence rate in one-dimensional space and multidimensional space on Cartesian meshes with piecewise tensor product polynomials of degree at most $k \geq 0$. By virtue of this kind of projection, the proof line in this paper has an important feature that the dual argument is abandoned and we do not worry about the regularity of dual problem, as the usual treatment in the finite element analysis for the elliptic problem and parabolic problem.

To clearly display the main idea of this technique, we start in this paper by assuming that the parameters involved in the numerical fluxes for the prime variable with respect to the convection part and the diffusion part are taken to be the same; see (2.8) and (2.16). Different to the DG method for hyperbolic equations, we have to overcome the difficulties coming from the auxiliary variables. To this end, we would like to construct new projections similar to the generalized Gauss–Radau projection in [20] to deal with the projection errors about auxiliary variables. Under the weaker assumption on the regularity of solutions, we establish again the optimal approximation properties for the corresponding projections. Besides, as that for the purely alternating numerical flux, there are some minor differences in the error estimate for the one- and multi-dimensional problems, in which the latter case requires making use of the superconvergence property of the projection. In the superconvergence analysis of the projection, we get a slight improvement that the regularity assumption [20] on the exact solution can be weakened a lot; see Lemma 3.6 in section 3.3.

After that, we will consider in section 4 the general numerical flux, i.e., the parameters involved in the numerical fluxes for the prime variable regarding the convection part and the diffusion part are independently chosen. It is an interesting problem to design a nice projection and analysis line to derive the optimal error estimate. The similar issue has been discussed in [8], where the purely alternating numerical flux is considered. The authors used the local Gauss–Radau projections to the prime variable and the nice combination of the prime variable and auxiliary variable, respectively, in order to completely eliminate those projection errors at element boundary points. In this paper, we will adopt a new projection based on the generalized Gauss–Radau projection, to achieve the same goal for the general cases.

The paper is organized as follows. In section 2, we present the LDG scheme using the generalized alternating numerical fluxes for one- and two-dimensional space. The stability and a priori error estimates in the L^2-norm are also stated in Theorem 2.3 and Theorem 2.4, respectively. Section 3 is devoted to proving Theorem 2.4. Specifically, we start in subsection 3.1 by showing the definitions of the generalized Gauss–Radau projections and presenting their optimal approximation properties. We proceed to prove Theorem 2.4 for the one-dimensional space in subsection 3.2 and for the two-dimensional space in subsection 3.3. We then move on to the discussion of issues related to these projections in subsection 3.4. In section 4, we extend the above work to the more general numerical fluxes and obtain the

satisfactory error estimates along the similar line by virtue of the generalized Gauss–Radau projection and its nice extensions. In section 5, we present some numerical experiments that confirm the sharpness of our theoretical results. Some concluding remarks are given in section 6. Finally, in the Appendix we provide the proof for a more technical identity about the projection.

2. The LDG scheme and main results

In this section, we follow [13] to present the detailed LDG schemes in one- and two-dimensional space, respectively.

2.1. **One-dimensional case.** In one-dimensional space, (1.1) can be expressed explicitly in the form

$$\frac{\partial u}{\partial t}+c\frac{\partial u}{\partial x}-d\frac{\partial^2 u}{\partial x^2}=f(x,t), \tag{2.1}$$

with the periodic boundary condition and the initial condition $u(x,0)=u_0(x)$, where $c\geq 0$ is assumed for simplicity. As the usual treatment, we would like to introduce the auxiliary variable $p=\sqrt{d}\frac{\partial u}{\partial x}$, and consider the equivalent first-order system

$$\frac{\partial u}{\partial t}+\frac{\partial h_u}{\partial x}=f,\qquad p+\frac{\partial h_p}{\partial x}=0, \tag{2.2}$$

where $(h_u,h_p)=(cu-\sqrt{d}p,-\sqrt{d}u)$ is the physical flux, and u is called the prime variable.

The so-called LDG method is to seek the approximation solutions of u and p for any time, in the discontinuous finite element space. Let $\Omega_h=\{I_i\}_{i=1}^N$ be the partition of $\Omega=(0,2\pi)$, where the element $I_i=(x_{i-1/2},x_{i+1/2})$ has the length $h_i=x_{i+1/2}-x_{i-1/2}$ for $i=1,...,N$, and $h=\max_{1\leq i\leq N}h_i$. Note that $x_{1/2}=0$ and $x_{N+1/2}=2\pi$. We assume Ω_h is quasi-uniform mesh in this paper, namely, there exists a fixed positive constant ν independent of h, such that $\nu h\leq h_i\leq h$ for any $i=1,\ldots,N$, as h goes to zero. The associated finite element space is defined as

$$V_h\equiv V_h^{(1)}\equiv\{v\in L^2(\Omega)\colon v|_{I_i}\in P^k(I_i),\forall I_i\in\Omega_h\}, \tag{2.3}$$

where $P^k(I_i)$ denotes the space of polynomials in I_i of degree at most $k\geq 0$. Note that the functions in V_h are allowed to have discontinuities across the element interfaces. As usual, at each element boundary point $x_{i+1/2}$ the jump is denoted by

$$[\![v]\!]_{i+\frac{1}{2}}=v^+_{i+\frac{1}{2}}-v^-_{i+\frac{1}{2}}, \tag{2.4}$$

and the weighted average is denoted by

$$v^{(\theta)}_{i+\frac{1}{2}}=\theta v^-_{i+\frac{1}{2}}+\widetilde{\theta}v^+_{i+\frac{1}{2}},\quad \text{with } \widetilde{\theta}=1-\theta, \tag{2.5}$$

where $v^-_{i+1/2}$ and $v^+_{i+1/2}$ are the traces from the left and right direction, respectively, and θ is the given parameter.

For the initial condition, we can take $u_h(0)$ as any suitable approximation of $u_0(x)$. In this paper, we simply take $u_h(0)=\pi_h^{(1\mathrm{d})}u_0$, where $\pi_h^{(1\mathrm{d})}\equiv\pi_h$ is the one-dimensional L^2-projection into V_h. To be specific, for any function $u\in L^2(\Omega)$,

the projection $\pi_h^{(1\mathrm{d})}u$ is defined as the unique function in V_h such that for any $1 \le i \le N$,

$$\int_{I_i} \left[\pi_h^{(1\mathrm{d})}u(x) - u(x)\right] v_h(x)\mathrm{d}x = 0, \quad v_h \in P^k(I_i). \tag{2.6}$$

Then, for any time $t \in (0, T]$, we seek the approximation solutions u_h and p_h both in the finite element space V_h, such that

$$\int_{I_i} \frac{\partial u_h}{\partial t} v_h \mathrm{d}x - \int_{I_i} h_u \frac{\partial v_h}{\partial x}\mathrm{d}x + (\hat{h}_u v_h^-)_{i+\frac{1}{2}} - (\hat{h}_u v_h^+)_{i-\frac{1}{2}} = \int_{I_i} f v_h \mathrm{d}x, \tag{2.7a}$$

$$\int_{I_i} p_h r_h \mathrm{d}x - \int_{I_i} h_p \frac{\partial r_h}{\partial x}\mathrm{d}x + (\hat{h}_p r_h^-)_{i+\frac{1}{2}} - (\hat{h}_p r_h^+)_{i-\frac{1}{2}} = 0, \tag{2.7b}$$

hold for any $i = 1, 2, \ldots, N$ and for any test function $(v_h, r_h) \in V_h \times V_h$. Here $(\hat{h}_u, \hat{h}_p)$ is the so-called numerical flux. Instead of using the purely alternating numerical fluxes, the novelty of this paper is to use the *generalized alternating* numerical fluxes related to an arbitrary parameter θ in a form

$$(\hat{h}_u, \hat{h}_p) = (cu_h^{(\theta)} - \sqrt{d}p_h^{(\tilde{\theta})}, -\sqrt{d}u_h^{(\theta)}) \tag{2.8}$$

at each element boundary point, where we have dropped the subscript $i + 1/2$ for convenience and $\theta \ge \frac{1}{2}$, since $c \ge 0$. The numerical flux defined in (2.8) is different from that appears in the literature [4, 6, 8], where $\theta = 1$, namely purely alternating numerical fluxes are used.

This completes the definition of the LDG scheme in one-dimensional space.

Remark 2.1. The parameters in the numerical flux regarding the convection part and diffusion part are not necessarily to be taken the same; see section 4. They can be chosen independently, and can be changed at different element boundary points. We take it as a constant in this paper just for simplicity.

2.2. **Two-dimensional case.** In two-dimensional space, (1.1) can be expressed explicitly in the form

$$\frac{\partial u}{\partial t} + c_1\frac{\partial u}{\partial x} + c_2\frac{\partial u}{\partial y} - d_1\frac{\partial^2 u}{\partial x^2} - d_2\frac{\partial^2 u}{\partial y^2} = f(x, y, t), \tag{2.9}$$

subject to the periodic boundary condition and the initial condition $u(x, y, 0) = u_0(x, y)$. For simplicity, assume $c_1 \ge 0$ and $c_2 \ge 0$. As the usual treatment, we would like to introduce the auxiliary variables

$$p = \sqrt{d_1}\frac{\partial u}{\partial x}, \quad q = \sqrt{d_2}\frac{\partial u}{\partial y},$$

and consider the equivalent first-order system

$$\frac{\partial u}{\partial t} + \frac{\partial h_{1u}}{\partial x} + \frac{\partial h_{2u}}{\partial y} = f, \quad p + \frac{\partial h_p}{\partial x} = 0, \quad q + \frac{\partial h_q}{\partial y} = 0, \tag{2.10}$$

where $(h_{1u}, h_p) = (c_1 u - \sqrt{d_1}p, -\sqrt{d_1}u)$ and $(h_{2u}, h_q) = (c_2 u - \sqrt{d_2}q, -\sqrt{d_2}u)$ are the physical fluxes.

The so-called LDG method is to seek the approximation solutions of u, p and q for any time, in the discontinuous finite element space. To do that, we would like to use some notations for triangulation and finite element space which are slightly different from the one-dimensional case. Let $\Omega_h = \{K_{ij}\}_{i=1,\ldots,N_x}^{j=1,\ldots,N_y}$ denote a tessellation of $\Omega = (0, 2\pi)^2$ with rectangular element $K_{ij} \equiv I_i \times J_j$, where $I_i =$

$(x_{i-1/2}, x_{i+1/2})$ and $J_j = (y_{j-1/2}, y_{j+1/2})$, with the length $h_i^x = x_{i+\frac{1}{2}} - x_{i-\frac{1}{2}}$ and width $h_j^y = y_{j+\frac{1}{2}} - y_{j-\frac{1}{2}}$. Let $h_{ij} = \max(h_i^x, h_j^y)$ and denote $h = \max_{K_{ij}\in\Omega_h} h_{ij}$. We also assume Ω_h is quasi-uniform in this paper, namely, there exists a fixed positive constant ν independent of h, such that $\nu h \le \min\{h_i^x, h_j^y\} \le h$ for any $i = 1, \ldots, N_x$ and $j = 1, \ldots, N_y$, as h goes to zero. The associated finite element space is defined as

$$V_h \equiv V_h^{(2)} \equiv \{v \in L^2(\Omega) : v|_K \in Q^k(K), \forall K \in \Omega_h\}, \tag{2.11}$$

where $Q^k(K)$ denotes the space of polynomials on K of degree at most $k \ge 0$ in each variable. Similar to the one-dimensional case, we use

$$[\![v]\!]_{i+1/2,y} = v^+_{i+1/2,y} - v^-_{i+1/2,y}, \quad [\![v]\!]_{x,j+1/2} = v^+_{x,j+1/2} - v^-_{x,j+1/2} \tag{2.12}$$

to denote the jumps on vertical and horizontal edges, where

$$v^{\pm}_{i+\frac{1}{2},y} = \lim_{x\to x_{i+\frac{1}{2}}\pm} v(x,y), \quad v^{\pm}_{x,j+\frac{1}{2}} = \lim_{y\to y_{j+\frac{1}{2}}\pm} v(x,y)$$

are the traces along two different directions. Here and below, we use

$$v^{\theta_1,y}_{i+\frac{1}{2},y} = \theta_1 v^-_{i+\frac{1}{2},y} + \widetilde{\theta}_1 v^+_{i+\frac{1}{2},y}, \quad v^{x,\theta_2}_{x,j+\frac{1}{2}} = \theta_2 v^-_{x,j+\frac{1}{2}} + \widetilde{\theta}_2 v^+_{x,j+\frac{1}{2}} \tag{2.13}$$

to represent the weighted averages on vertical and horizontal edges with $\widetilde{\theta}_1 = 1-\theta_1$ and $\widetilde{\theta}_2 = 1-\theta_2$.

For the initial condition, we can take $u_h(0)$ as the suitable approximation of $u_0(x,y)$. In this paper, we simply take $u_h(0) = \pi_h^{(2\mathrm{d})} u_0$, where $\pi_h^{(2\mathrm{d})} = \pi_h^x \otimes \pi_h^y$ is the two-dimensional L^2-projection into V_h. Here and below the superscripts x and y indicate that the one-dimensional projections are applied to the spatial variables x and y, respectively. That is, for any function $u \in L^2(\Omega)$, the projection $\pi_h^{(2\mathrm{d})} u$ is defined as the unique function in V_h such that, in each $K_{ij} \in \Omega_h$,

$$\int_{K_{ij}} \Big[\pi_h^{(2\mathrm{d})} u(x,y) - u(x,y)\Big] v_h(x,y)\mathrm{d}x\mathrm{d}y = 0, \quad v_h \in Q^k(K_{ij}). \tag{2.14}$$

Then, for any time $t \in (0,T]$, we seek the approximation solutions u_h, p_h and q_h in the finite element space V_h, such that, in each $K_{ij} \in \Omega_h$,

$$\begin{aligned}
&\int_{K_{ij}} \Big[\frac{\partial u_h}{\partial t} v_h - h_{1u}\frac{\partial v_h}{\partial x} - h_{2u}\frac{\partial v_h}{\partial y}\Big]\mathrm{d}x\mathrm{d}y \\
&\qquad + \int_{J_j} \Big[(\hat{h}_{1u} v_h^-)_{i+\frac{1}{2},y} - (\hat{h}_{1u} v_h^+)_{i-\frac{1}{2},y}\Big]\mathrm{d}y \\
&\qquad + \int_{I_i} \Big[(\hat{h}_{2u} v_h^-)_{x,j+\frac{1}{2}} - (\hat{h}_{2u} v_h^+)_{x,j-\frac{1}{2}}\Big]\mathrm{d}x = \int_{K_{ij}} f v_h \mathrm{d}x\mathrm{d}y,
\end{aligned} \tag{2.15a}$$

$$\int_{K_{ij}} \Big[p_h r_h - h_p \frac{\partial r_h}{\partial x}\Big]\mathrm{d}x\mathrm{d}y + \int_{J_j} \Big[(\hat{h}_p r_h^-)_{i+\frac{1}{2},y} - (\hat{h}_p r_h^+)_{i-\frac{1}{2},y}\Big]\mathrm{d}y = 0, \tag{2.15b}$$

$$\int_{K_{ij}} \Big[q_h s_h - h_q \frac{\partial s_h}{\partial y}\Big]\mathrm{d}x\mathrm{d}y + \int_{I_i} \Big[(\hat{h}_q s_h^-)_{x,j+\frac{1}{2}} - (\hat{h}_q s_h^+)_{x,j-\frac{1}{2}}\Big]\mathrm{d}x = 0, \tag{2.15c}$$

hold for all test function $(v_h, r_h, s_h) \in V_h \times V_h \times V_h$. Similar to the one-dimensional case, the numerical fluxes $(\hat{h}_{1u}, \hat{h}_p)$ and $(\hat{h}_{2u}, \hat{h}_q)$ are defined in a *generalized alternating* form with respect to each spatial direction, namely

$$(\hat{h}_{1u}, \hat{h}_p) = \Big(c_1 u_h^{\theta_1,y} - \sqrt{d} p_h^{\widetilde{\theta_1},y}, -\sqrt{d} u_h^{\theta_1,y}\Big), \tag{2.16a}$$

$$(\hat{h}_{2u}, \hat{h}_q) = \Big(c_2 u_h^{x,\theta_2} - \sqrt{d} q_h^{x,\widetilde{\theta_2}}, -\sqrt{d} u_h^{x,\theta_2}\Big) \tag{2.16b}$$

on the vertical and horizontal edges, respectively, where $\theta_1 \geq 1/2$ and $\theta_2 \geq 1/2$ are the given parameters, since $c_1 \geq 0$ and $c_2 \geq 0$. Note that we have dropped the subscripts for convenience.

This completes the definition of the LDG scheme in two-dimensional space.

2.3. **Main results.** In this subsection we would like to present the stability and optimal error estimates in the L^2-norm.

2.3.1. *Compact representations.* For notational convenience, we would like to rewrite the above LDG schemes into a compact form, respectively.

For example, adding up two equations in (2.7) and summing them over all elements, the LDG scheme (2.7) in the one-dimensional space can be written in the form: find $(u_h, p_h) \in V_h \times V_h$ for any time $t \in (0, T]$, such that

$$\int_\Omega \frac{\partial u_h}{\partial t} v_h \mathrm{d}x + G_h(u_h, p_h; v_h, r_h) = \int_\Omega f v_h \mathrm{d}x \tag{2.17}$$

for any test function $(v_h, r_h) \in V_h \times V_h$, where

$$\begin{aligned} G_h(u_h, p_h; v_h, r_h) &= \int_\Omega p_h r_h \mathrm{d}x \\ &\quad + \sum_{i=1}^{N} \Big\{ -c H_i^{(\theta)}(u_h, v_h) + \sqrt{d} H_i^{(\widetilde{\theta})}(p_h, v_h) + \sqrt{d} H_i^{(\theta)}(u_h, r_h) \Big\} \end{aligned} \tag{2.18}$$

with the locally-defined functional for the given parameter α,

$$H_i^{(\alpha)}(w, z) = \int_{I_i} w \frac{\partial z}{\partial x} \mathrm{d}x - (w^{(\alpha)} z^-)_{i+\frac{1}{2}} + (w^{(\alpha)} z^+)_{i-\frac{1}{2}}.$$

Similarly, the LDG scheme (2.15) in two-dimensional space can be written into the following compact form: find $(u_h, p_h, q_h) \in V_h \times V_h \times V_h$ for any time $t \in (0, T]$, such that

$$\int_\Omega \frac{\partial u_h}{\partial t} v_h \mathrm{d}x\mathrm{d}y + G_h(u_h, p_h, q_h; v_h, r_h, s_h) = \int_\Omega f v_h \mathrm{d}x\mathrm{d}y \tag{2.19}$$

for any test function $(v_h, r_h, s_h) \in V_h \times V_h \times V_h$, where

$$\begin{aligned} G_h(u_h, p_h, q_h; v_h, r_h, s_h) &= \int_\Omega p_h r_h \mathrm{d}x\mathrm{d}y + \int_\Omega q_h s_h \mathrm{d}x\mathrm{d}y \\ &\quad + \sum_{i=1}^{N_x} \sum_{j=1}^{N_y} \Big\{ - c_1 H_{ij}^{1,\theta_1}(u_h, v_h) + \sqrt{d_1} H_{ij}^{1,\widetilde{\theta_1}}(p_h, v_h) + \sqrt{d_1} H_{ij}^{1,\theta_1}(u_h, r_h) \Big\} \\ &\quad + \sum_{i=1}^{N_x} \sum_{j=1}^{N_y} \Big\{ - c_2 H_{ij}^{2,\theta_2}(u_h, v_h) + \sqrt{d_2} H_{ij}^{2,\widetilde{\theta_2}}(q_h, v_h) + \sqrt{d_2} H_{ij}^{2,\theta_2}(u_h, s_h) \Big\} \end{aligned} \tag{2.20}$$

with the locally-defined functionals for the given parameters α_1 and α_2,

$$H_{ij}^{1,\alpha_1}(w,z)=\int_{K_{ij}} w\frac{\partial z}{\partial x}\mathrm{d}x\mathrm{d}y-\int_{J_j}\Big[(w^{\alpha_1,y}z^-)_{i+\frac{1}{2},y}-(w^{\alpha_1,y}z^+)_{i-\frac{1}{2},y}\Big]\mathrm{d}y,$$
$$H_{ij}^{2,\alpha_2}(w,z)=\int_{K_{ij}} w\frac{\partial z}{\partial y}\mathrm{d}x\mathrm{d}y-\int_{I_i}\Big[(w^{x,\alpha_2}z^-)_{x,j+\frac{1}{2}}-(w^{x,\alpha_2}z^+)_{x,j-\frac{1}{2}}\Big]\mathrm{d}x.$$

2.3.2. *Stability.* In the discontinuous finite element method, the information on the element boundaries is important. To be convenient, we would like to use Γ_h to denote all element boundary points in one-dimensional space, and use Γ_h^x and Γ_h^y to denote all vertical edges and all horizontal edges of element boundaries in two-dimensional space, respectively. Furthermore, we use

$$\|v\|_{L^2(\Gamma_h)}=\left(\frac{1}{2}\sum_{i=1}^{N}\Big[(v^+)^2_{i-\frac{1}{2}}+(v^-)^2_{i+\frac{1}{2}}\Big]\right)^{\frac{1}{2}},\tag{2.21a}$$

$$\|v\|_{L^2(\Gamma_h^x)}=\left(\frac{1}{2}\sum_{i=1}^{N_x}\sum_{j=1}^{N_y}\int_{J_j}\Big[(v^+)^2_{i-\frac{1}{2},y}+(v^-)^2_{i+\frac{1}{2},y}\Big]\mathrm{d}y\right)^{\frac{1}{2}},\tag{2.21b}$$

$$\|v\|_{L^2(\Gamma_h^y)}=\left(\frac{1}{2}\sum_{i=1}^{N_x}\sum_{j=1}^{N_y}\int_{I_i}\Big[(v^+)^2_{x,j-\frac{1}{2}}+(v^-)^2_{x,j+\frac{1}{2}}\Big]\mathrm{d}x\right)^{\frac{1}{2}},\tag{2.21c}$$

for any function v defined on element boundaries. If v is single-valued there, we can define $v^+=v^-=v$. Note that the notations in (2.21) depend on the used mesh.

It is trivial to get the L^2-norm stability of the above LDG schemes by noticing the following identities:

$$G_h(u_h,p_h;u_h,p_h)=\|p_h\|^2+c\Big(\theta-\frac{1}{2}\Big)\|[\![u_h]\!]\|^2_{L^2(\Gamma_h)}\tag{2.22a}$$

for the one-dimensional space, and

$$\begin{aligned}&G_h(u_h,p_h,q_h;u_h,p_h,q_h)\\&=\|p_h\|^2+\|q_h\|^2+c_1(\theta_1-\frac{1}{2})\|[\![u_h]\!]\|^2_{L^2(\Gamma_h^x)}+c_2(\theta_2-\frac{1}{2})\|[\![u_h]\!]\|^2_{L^2(\Gamma_h^y)}\end{aligned}\tag{2.22b}$$

for two-dimensional space, where an unmarked norm $\|\cdot\|$ is the usual L^2-norm defined on the whole domain Ω. Note that $[\![u_h]\!]$ is a single-valued function on element boundaries. Since the proofs of (2.22) follow from the simple manipulations or the same arguments as that in [13], we omit the details here.

Remark 2.2. The above two identities show that the jumps of auxiliary variables do not provide any contributions to the numerical stability. For example, for the one-dimensional pure heat equation (i.e., $c=0$), the corresponding LDG scheme only has one stability term $\|p_h\|^2$ in (2.22a). This is an important difference between the LDG method and the interior penalty methods [22] for steady problem.

Theorem 2.3. *The one-dimensional LDG scheme* (2.7) *with* $\theta\geq\frac{1}{2}$*, and the two-dimensional LDG scheme* (2.15) *with* $\theta_1,\theta_2\geq\frac{1}{2}$ *are both stable in the* L^2*-norm, namely, the numerical solution satisfies*

$$\|u_h(T)\|\leq\|u_h(0)\|+\int_0^T\|f(t)\|\,\mathrm{d}t.\tag{2.23}$$

Proof. Let us take the one-dimensional case as an example. Taking the test function $(v_h, r_h) = (u_h, p_h)$ in (2.17), and using (2.22a) and Cauchy–Schwarz inequality, we can easily get

$$\frac{1}{2}\frac{\mathrm{d}}{\mathrm{d}t}\|u_h\|^2 \le \|f\|\,\|u_h\|\,. \tag{2.24}$$

The L^2-norm stability (2.23) follows immediately by canceling $\|u_h\|$ on both sides and integrating the inequality with respect to the time between 0 and T.

Proceeding in a similar way, we can also obtain (2.23) for the two-dimensional space. This finishes the proof. □

2.3.3. *Error estimates.* Now we state the optimal a priori error estimates of the above LDG method based on the generalized alternating numerical fluxes (2.8) and (2.16), respectively, where the usual Sobolev spaces and Bochner spaces as well as their norms and notations are used. If the space domain is Ω, and/or the time interval is $[0, T]$, we will omit them for convenience.

Theorem 2.4. *Assume that the exact solution of* (1.1) *is sufficiently smooth, i.e.*

$$u \in L^\infty(H^{k+1}) \cap L^2(H^{k+2}), \quad \frac{\partial u}{\partial t} \in L^2(H^{k+1}). \tag{2.25}$$

If the discontinuous finite element space V_h is made up of piecewise polynomials of degree $k \ge 0$ in each variable, defined on the quasi-uniform Cartesian mesh, then the numerical solution u_h, of either the one-dimensional LDG scheme (2.7) *with $\theta > 1/2$, or of the two-dimensional LDG scheme* (2.15) *with $\theta_1 > 1/2$ and $\theta_2 > 1/2$, satisfies the optimal and uniform error estimate*

$$\|u(T) - u_h(T)\| \le C(1+T)h^{k+1}, \tag{2.26}$$

where the bounding constant C is independent of mesh size h and the reciprocal of the diffusion coefficient d.

Before we present the proof of this theorem in the next section, we would like to give some remarks here.

Remark 2.5. The above optimal error estimate has been established in the literature for some special θ. For example, the numerical flux (2.8) in the one-dimensional LDG scheme can be rewritten in the form as [13], namely,

$$\begin{bmatrix} \widehat{h}_u \\ \widehat{h}_p \end{bmatrix} = \begin{bmatrix} c u_h^{(\frac{1}{2})} - \beta_{00}[\![u_h]\!] \\ 0 \end{bmatrix} + \begin{bmatrix} -\sqrt{d} p_h^{(\frac{1}{2})} - \beta_{11}[\![u_h]\!] - \beta_{12}[\![p_h]\!] \\ -\sqrt{d} u_h^{(\frac{1}{2})} + \beta_{12}[\![u_h]\!] \end{bmatrix}, \tag{2.27}$$

with $\beta_{00} = (\theta - \frac{1}{2})c$, as well as $\beta_{11} = 0$ and $\beta_{12} = (\theta - \frac{1}{2})\sqrt{d}$. However, only suboptimal convergence result of order k is obtained for arbitrary parameter θ by using the local L^2-projection π_h in [13]. The authors also reported numerically the optimal convergence rate for the purely alternating numerical fluxes, namely $\theta = 1$, which is proved in [6] by the aid of the local Gauss–Radau projection.

It is worthy to point out that one cannot derive the optimal L^2-norm error estimate for $\beta_{11} = 0$ and general numerical fluxes, even we use the dual argument as [5], as well as the local L^2-projection or local Gauss–Radau projection. The restriction $\beta_{11} = \mathcal{O}(h^{-1})$ is critically used in [5] to obtain the optimal L^2-norm error estimate, when the LDG method is used to solve the pure elliptic equation. However, owing to the generalized Gauss–Radau projection, we are able to get rid

of the dual arguments and prove directly the optimal convergence rate for general numerical fluxes, as the actual numerical experiments show.

Remark 2.6. Some remarks will be given in section 3.4, when the parameter used in the numerical flux is equal to one half.

Remark 2.7. The conclusion in Theorem 2.4 can be extended easily to three-dimensional space. The proof line is almost the same as that in two-dimensional space, as long as the exact solution is smooth enough to ensure its continuity.

3. Proof of Theorem 2.4

In this section we will prove Theorem 2.4, no matter how small the diffusion coefficient d is. The main technique is the construction and analysis of some generalized Gauss–Radau projections [20] and their extensions. However, there is a little difference between the one-dimensional space and multi-dimensional space.

For notational convenience, below we would like to use C to denote a generic constant independent of h and d^{-1}, which may have a different value in each occurrence.

3.1. Generalized Gauss–Radau projections.

In what follows we would like to consider the functions in the broken Sobolev space

$$H^\ell(\Omega_h) = \{z \in L^2(\Omega) : z|_K \in H^\ell(K), \forall K \in \Omega_h\} \tag{3.1}$$

equipped with the norm $\|z\|_{H^\ell(\Omega_h)} = \Big(\sum_{K\in\Omega_h} \|z\|^2_{H^\ell(K)}\Big)^{1/2}$, for any given integer $\ell \geq 0$. Moreover, we denote by $C(\bar{\Omega}_h)$ the space made up of all piecewise continuous functions. Since the discontinuous finite element space V_h is contained and dense in the above two spaces, as h goes to zero, those notations in the previous section can be extended as usual.

3.1.1. *Elemental projection in one-dimensional space.* Assume $\theta \neq \frac{1}{2}$, and we define the generalized Gauss–Radau projection as [20]. Namely, for any periodic function $z \in C(\bar{\Omega}_h)$, the projection $P_\theta z \in V_h$ satisfies

$$\int_{I_i} (P_\theta z) v_h \mathrm{d}x = \int_{I_i} z v_h \mathrm{d}x, \quad \forall v_h \in P^{k-1}(I_i), \tag{3.2a}$$

$$(P_\theta z)^{(\theta)}_{i+\frac{1}{2}} = (z^{(\theta)})_{i+\frac{1}{2}} \tag{3.2b}$$

for any $i = 1, \ldots, N$. Obviously, this projection degenerates to the local Gauss–Radau projection if the parameter is taken as 0 or 1. Hence it can be viewed as an extension of the local Gauss–Radau projections.

Remark 3.1. In particular, for $k = 0$, the condition (3.2a) is vacuous. Likewise for other projections in this paper.

The unique existence has been discussed in [20], and the optimal approximation properties have been obtained for those functions in $W^{k+1,\infty}(\Omega_h)$, in which the derivatives up to $(k+1)$-th order are bounded in each element. However, we would like in this paper to improve regularity assumption to coincide with the traditional requirement, as [19], by the help of the special construction of a matrix and the well-known approximation property of local L^2-projection.

Lemma 3.2. *Assume $z \in H^{s+1}(\Omega_h)$ with $\Omega_h \subset \mathbb{R}^1$ and $s \geq 0$. For $\theta \neq \frac{1}{2}$, the projection $P_\theta z$ is well-defined and the projection error $\eta = z - P_\theta z$ satisfies*

$$\|\eta\|_{L^2(\Omega_h)} + h^{\frac{1}{2}} \|\eta\|_{L^2(\Gamma_h)} \leq C h^{\min(k+1,s+1)} \|z\|_{H^{s+1}(\Omega_h)}, \tag{3.3}$$

where the bounding constant $C > 0$ is independent of h and z.

Proof. Since $z \in H^1(\Omega_h)$, the imbedding theorem implies that the point value is defined well. Hence the expression in (3.2) is reasonable.

Let $E = P_\theta z - \pi_h z$, where $\pi_h = \pi_h^{(1\mathrm{d})}$ is the one-dimensional L^2-projection defined in (2.6). Obviously, it satisfies for any $i = 1, \ldots, N$, the following conditions

$$\int_{I_i} E v_h \mathrm{d}x = 0, \quad \forall v_h \in P^{k-1}(I_i), \tag{3.4a}$$

$$E^{(\theta)}_{i+\frac{1}{2}} = (z - \pi_h z)^{(\theta)}_{i+\frac{1}{2}} \equiv b_i. \tag{3.4b}$$

It is well-known that $\pi_h z$ exists uniquely and satisfies the approximation property

$$\|z - \pi_h z\|_{L^2(I_i)} + h_i^{\frac{1}{2}} \|z - \pi_h z\|_{L^\infty(I_i)} \leq C h_i^{\min(k+1,s+1)} \|z\|_{H^{s+1}(I_i)}, \tag{3.5}$$

in each element I_i, where the bounding constant C is independent of i and z. To prove this lemma, we just need to show that $E \in V_h$ exists uniquely and satisfies the following approximation property

$$\|E\|_{L^2(\Omega_h)} + h^{\frac{1}{2}} \|E\|_{L^2(\Gamma_h)} \leq C h^{\min(k+1,s+1)} \|z\|_{H^{s+1}(\Omega_h)}. \tag{3.6}$$

These aims can be achieved by direct manipulations. Due to (3.4a) and the orthogonality of the rescaled Legendre polynomials, it is easy to see that

$$E(x) = \alpha_{i,k} P_{i,k}(x) = \alpha_{i,k} \hat{P}_k(\hat{x}),$$

in each element I_i, with $\hat{x} = 2(x - x_i)/h_i$. Here and below

$$P_{i,l}(x) \equiv \widehat{P}_l\Big(\frac{2(x - x_i)}{h_i}\Big) \equiv \widehat{P}_l(\hat{x}),$$

and $\widehat{P}_l(\hat{x})$ is the standard Legendre polynomial of degree l defined on $[-1, 1]$. Since $\widehat{P}_k(\pm 1) = (\pm 1)^k$, it follows from (3.4b) that

$$\theta \alpha_{i,k} + \widetilde{\theta}(-1)^k \alpha_{i+1,k} = b_i, \quad i = 1, \cdots, N. \tag{3.7}$$

Note that $\alpha_{N+1,k} = \alpha_{1,k}$. In other words, it forms a linear system $\mathbb{A}_N \vec{\alpha}_N = \vec{b}_N$ to determine $\vec{\alpha}_N = (\alpha_{1,k}, \alpha_{2,k}, \ldots, \alpha_{N,k})^\top$, where $\vec{b}_N = (b_1, b_2, \ldots, b_N)^\top$. It is easy to work out that

$$\det(\mathbb{A}_N) = \theta^N (1 - \zeta^N), \quad \text{with } \zeta = (-1)^{k+1} \widetilde{\theta}/\theta. \tag{3.8}$$

Hence $\det(\mathbb{A}_N) \neq 0$ and the matrix $\mathbb{A}_N$ is invertible provided that $\theta \neq 1/2$. Now we can conclude that E and thus the projection $P_\theta z$ is determined uniquely.

A deep manipulation as that in [20] yields the special construction of the inverse matrix. That is, $\mathbb{A}_N^{-1}$ is a circulant matrix with the (i, j)-th entry

$$(\mathbb{A}_N^{-1})_{ij} = \frac{1}{\theta(1 - \zeta^N)} \zeta^{\mathrm{mod}(j-i,N)}.$$

It is easy to see [16] that the row-norm and column-norm are equal and satisfy

$$\left\|\mathbb{A}_N^{-1}\right\|_1 = \left\|\mathbb{A}_N^{-1}\right\|_\infty \le \frac{1}{|\theta||1-\zeta^N|}\frac{|1-|\zeta|^N|}{|1-|\zeta||} \le \frac{1}{|\theta||1-|\zeta||},$$

hence the spectral norm satisfies

$$\left\|\mathbb{A}_N^{-1}\right\|_2^2 \le \left\|\mathbb{A}_N^{-1}\right\|_1 \left\|\mathbb{A}_N^{-1}\right\|_\infty \le \frac{1}{\theta^2(1-|\zeta|)^2}. \tag{3.9}$$

It is worthy to mention that this inequality holds independently of N. Owing to the approximation property (3.5), we have

$$\begin{aligned}\|\vec{\alpha}_N\|_2^2 =& \left\|\mathbb{A}_N^{-1}\vec{b}_N\right\|_2^2 \le \left\|\mathbb{A}_N^{-1}\right\|_2^2 \left\|\vec{b}_N\right\|_2^2 \le C\left\|\vec{b}_N\right\|_2^2 \\ &\le C\left\|z-\pi_h z\right\|_{\Gamma_h}^2 \le Ch^{2\min(k+1,s+1)-1}\left\|z\right\|_{H^{s+1}(\Omega_h)}^2,\end{aligned} \tag{3.10}$$

where the bounding constant $C > 0$ is independent of h. Finally, noticing the simple fact

$$\|E\|_{L^2(\Omega_h)}^2 = \sum_{i=1}^N \alpha_{i,k}^2 \left\|P_{i,k}(x)\right\|_{L^2(I_i)}^2 = \sum_{i=1}^N \frac{h_i\alpha_{i,k}^2}{2k+1} \le Ch\left\|\vec{\alpha}_N\right\|_2^2, \tag{3.11a}$$

$$\|E\|_{L^2(\Gamma_h)}^2 = \sum_{i=1}^N \alpha_{i,k}^2 = \left\|\vec{\alpha}_N\right\|_2^2, \tag{3.11b}$$

as well as (3.10), we can obtain (3.6) and finish the proof of this lemma. □

3.1.2. *Elemental projection in multi-dimensional space.* It is easy to define the generalized Gauss–Radau projection in multi-dimensional space ($m = 2$ or $m = 3$). To save space, below we would like to present only the projection in two-dimensional space.

Assume that $\theta_1 \ne \frac{1}{2}$ and $\theta_2 \ne \frac{1}{2}$. The projection P_{θ_1,θ_2} can be explained as the tensor product of the one-dimensional projections P_θ^x and P_θ^y, in x- and y-direction respectively, namely,

$$P_{\theta_1,\theta_2} = P_{\theta_1}^x \otimes P_{\theta_2}^y. \tag{3.12}$$

To be specific, for any periodic function $z \in C(\bar{\Omega}_h)$, the projection $P_{\theta_1,\theta_2}z \in V_h$ satisfies

$$\int_{K_{ij}} (P_{\theta_1,\theta_2}z)v_h \mathrm{d}x\mathrm{d}y = \int_{K_{ij}} zv_h \mathrm{d}x\mathrm{d}y, \quad \forall v_h \in Q^{k-1}(K_{ij}), \tag{3.13a}$$

$$\int_{J_j} \left((P_{\theta_1,\theta_2}z)^{\theta_1,y}v_h\right)_{i+\frac{1}{2},y} \mathrm{d}y = \int_{J_j} \left(z^{\theta_1,y}v_h\right)_{i+\frac{1}{2},y} \mathrm{d}y, \quad \forall v_h \in P^{k-1}(J_j), \tag{3.13b}$$

$$\int_{I_i} \left((P_{\theta_1,\theta_2}z)^{x,\theta_2}v_h\right)_{x,j+\frac{1}{2}} \mathrm{d}x = \int_{I_i} \left(z^{x,\theta_2}v_h\right)_{x,j+\frac{1}{2}} \mathrm{d}x, \quad \forall v_h \in P^{k-1}(I_i), \tag{3.13c}$$

$$\left(P_{\theta_1,\theta_2}z\right)_{i+\frac{1}{2},j+\frac{1}{2}}^{\theta_1,\theta_2} = z_{i+\frac{1}{2},j+\frac{1}{2}}^{\theta_1,\theta_2} \tag{3.13d}$$

for any $i = 1,\dots,N_x$ and $j = 1,\dots,N_y$. Here and in what follows, we use the notations defined in (2.13) to represent the weighted average on each edge, and use

$$\begin{aligned}z_{i+\frac{1}{2},j+\frac{1}{2}}^{\theta_1,\theta_2} =& \theta_1\theta_2 z(x_{i+\frac{1}{2}}^-, y_{j+\frac{1}{2}}^-) + \theta_1\widetilde{\theta}_2 z(x_{i+\frac{1}{2}}^-, y_{j+\frac{1}{2}}^+) \\ &+ \widetilde{\theta}_1\theta_2 z(x_{i+\frac{1}{2}}^+, y_{j+\frac{1}{2}}^-) + \widetilde{\theta}_1\widetilde{\theta}_2 z(x_{i+\frac{1}{2}}^+, y_{j+\frac{1}{2}}^+)\end{aligned} \tag{3.14}$$

to represent the weighted average at the corner point.

Almost the same as the discussion for the one-dimensional projection, we have the following approximation property.

Lemma 3.3. *Assume $z \in H^{s+1}(\Omega_h) \cap H^2(\Omega_h)$ with $\Omega_h \subset \mathbb{R}^2$ and $s \geq 0$. For $\theta_1 \neq \frac{1}{2}$ and $\theta_2 \neq \frac{1}{2}$, the projection $P_{\theta_1,\theta_2} z$ is well-defined and the projection error $\eta = z - P_{\theta_1,\theta_2} z$ satisfies*

$$\|\eta\|_{L^2(\Omega_h)} + h^{\frac{1}{2}} \|\eta\|_{L^2(\Gamma_h)} \leq C h^{\min(k+1,s+1)} \|z\|_{H^{s+1}(\Omega_h)}, \tag{3.15}$$

where $\|\eta\|^2_{L^2(\Gamma_h)} = \|\eta\|^2_{L^2(\Gamma_h^x)} + \|\eta\|^2_{L^2(\Gamma_h^y)}$, and the bounding constant $C > 0$ is independent of h and z.

Proof. Since $z \in H^2(\Omega_h)$, the imbedding theorem implies that the point value is defined well. Hence the expression in (3.13) is reasonable.

The proof idea is almost the same as that for the one-dimensional case. However, the procedure is a little long and complex. Let $E = P_{\theta_1,\theta_2} z - \pi_h z$, where $\pi_h = \pi_h^{(2\mathrm{d})}$ is the two-dimensional L^2-projection defined in (2.14). Obviously, $E \in V_h$ satisfies the following identities

$$\int_{K_{i,j}} E v_h \mathrm{d}x\mathrm{d}y = 0, \quad \forall v_h \in Q^{k-1}(K_{ij}), \tag{3.16a}$$

$$\int_{J_j} \left(E^{\theta_1,y} v_h\right)_{i+\frac{1}{2},y} \mathrm{d}y = \int_{J_j} \left(g^{\theta_1,y} v_h\right)_{i+\frac{1}{2},y} \mathrm{d}y, \quad \forall v_h \in P^{k-1}(J_j), \tag{3.16b}$$

$$\int_{I_i} \left(E^{x,\theta_2} v_h\right)_{x,j+\frac{1}{2}} \mathrm{d}x = \int_{I_i} \left(g^{x,\theta_2} v_h\right)_{x,j+\frac{1}{2}} \mathrm{d}x, \quad \forall v_h \in P^{k-1}(I_i), \tag{3.16c}$$

$$E^{\theta_1,\theta_2}_{i+\frac{1}{2},j+\frac{1}{2}} = g^{\theta_1,\theta_2}_{i+\frac{1}{2},j+\frac{1}{2}}, \tag{3.16d}$$

for any $i = 1, 2, \ldots, N_x$ and $j = 1, 2, \ldots, N_y$, where $g = z - \pi_h^{(2\mathrm{d})} z$ is already known and satisfies

$$\|g\|_{L^2(K_{ij})} + h_{ij} \|g\|_{L^\infty(K_{ij})} \leq C h_{ij}^{\min(k+1,s+1)} \|z\|_{H^{s+1}(K_{ij})}, \tag{3.17}$$

in each element K_{ij}. Here the bounding constant C is independent of i, j and z. To prove this lemma, we just need to show that $E \in V_h$ exists uniquely and satisfies the following approximation property

$$\|E\|_{L^2(\Omega_h)} + h^{\frac{1}{2}} \|E\|_{L^2(\Gamma_h)} \leq C h^{\min(k+1,s+1)} \|z\|_{H^{s+1}(\Omega_h)}. \tag{3.18}$$

These aims can be achieved by direct manipulations. Due to (3.16a) and the orthogonality of the rescaled Legendre polynomials in each rectangle, it is easy to see that $E = E_x + E_y + E_{xy}$, with the following expressions

$$E_x = \sum_{l_2=0}^{k-1} \alpha_{i,j,k,l_2} P_{i,k}(x) P_{j,l_2}(y) = \sum_{l_2=0}^{k-1} \alpha_{i,j,k,l_2} \hat{P}_k(\hat{x}) \hat{P}_{l_2}(\hat{y}), \tag{3.19a}$$

$$E_y = \sum_{l_1=0}^{k-1} \alpha_{i,j,l_1,k} P_{i,l_1}(x) P_{j,k}(y) = \sum_{l_1=0}^{k-1} \alpha_{i,j,l_1,k} \hat{P}_{l_1}(\hat{x}) \hat{P}_k(\hat{y}), \tag{3.19b}$$

$$E_{xy} = \alpha_{i,j,k,k} P_{i,k}(x) P_{j,k}(y) = \alpha_{i,j,k,k} \hat{P}_k(\hat{x}) \hat{P}_k(\hat{y}), \tag{3.19c}$$

in each element K_{ij}. Here $\hat{x} = 2(x - x_i)/h_i^x$ and $\hat{y} = 2(y - y_j)/h_j^y$, with (x_i, y_j) being the central point of K_{ij}.

The unique existence and approximation properties about E_x, E_y and E_{xy} will be shown by a similar procedure. For example, along the analogous line as that in Lemma 3.2, we can solve out E_x by the following linear system

$$\theta_1 \alpha_{i,j,k,l_2} + (-1)^k \widetilde{\theta}_1 \alpha_{i+1,j,k,l_2} = b_{i,j,k,l_2}, \quad i = 1, \ldots, N_x, \tag{3.20}$$

for any $j = 1, \cdots, N_y$ and any $l_2 = 0, \cdots, k-1$, where

$$\begin{aligned} b_{i,j,k,l_2} &\equiv \frac{1}{\|P_{j,l_2}\|^2_{L^2(J_j)}} \int_{J_j} \left(g^{\theta_1, y} P_{j,l_2}(y) \right)_{i+\frac{1}{2},y} \mathrm{d}y \\ &\leq \frac{\left\| g^{\theta_1,y}_{i+\frac{1}{2},y} \right\|_{L^2(J_j)}}{\|P_{j,l_2}\|_{L^2(J_j)}} = \sqrt{\frac{2l_2+1}{h_j^y}} \left\| g^{\theta_1,y}_{i+\frac{1}{2},y} \right\|_{L^2(J_j)} \\ &\leq C \left\| g^{\theta_1,y}_{i+\frac{1}{2},y} \right\|_{L^\infty(J_j)} \leq C \|g\|_{L^\infty(K_{ij} \cup K_{i+1,j})} . \end{aligned} \tag{3.21}$$

The associated matrix is nothing but $\mathbb{A}_{N_x}$, which is invertible if $\theta_1 \neq 1/2$. Hence, we can conclude that α_{i,j,k,l_2} exists uniquely for any $i = 1, \ldots, N_x$, and there holds

$$\sum_{i=1}^{N_x} \alpha^2_{i,j,k,l_2} \leq C \sum_{i=1}^{N_x} b^2_{i,j,k,l_2}, \tag{3.22}$$

for any $j = 1, \ldots, N_y$ and any $l_2 = 0, \ldots, k-1$. Then it follows from (3.21) and (3.22) that

$$\begin{aligned} \Sigma_x &\equiv \sum_{j=1}^{N_y} \sum_{l_2=0}^{k-1} \sum_{i=1}^{N_x} \alpha^2_{i,j,k,l_2} \leq C \sum_{j=1}^{N_y} \sum_{i=1}^{N_x} \|g\|^2_{L^\infty(K_{ij} \cup K_{i+1,j})} \\ &\leq C \sum_{j=1}^{N_y} \sum_{i=1}^{N_x} h_{ij}^{2\min(s,k)} \|z\|^2_{H^{s+1}(K_{ij})} \leq C h^{2\min(s,k)} \|z\|^2_{H^{s+1}(\Omega_h)} , \end{aligned} \tag{3.23}$$

where we have used (3.17). Repeating this process for another spatial direction, we can determine uniquely E_y and obtain a similar conclusion

$$\Sigma_y \equiv \sum_{i=1}^{N_x} \sum_{l_1=0}^{k-1} \sum_{j=1}^{N_y} \alpha^2_{i,j,l_1,k} \leq C h^{2\min(s,k)} \|z\|^2_{H^{s+1}(\Omega_h)} , \tag{3.24}$$

by help of the matrix $\mathbb{A}_{N_y}$.

The undetermined coefficients $\alpha_{i,j,k,k}$ in the last component E_{xy} can be solved out from the linear system in which the matrix $\mathbb{A}_{N_x} \otimes \mathbb{A}_{N_y}$ is invertible if $\theta_1 \neq 1/2$ and $\theta_2 \neq 1/2$, and the component in the right-hand vector is

$$b_{i,j,k,k} = (g - E_x - E_y)^{\theta_1,\theta_2}_{i+\frac{1}{2},j+\frac{1}{2}}, \quad i = 1, \ldots, N_x, j = 1, \ldots, N_y.$$

Since $\left\|(\mathbb{A}_{N_x}\otimes\mathbb{A}_{N_y})^{-1}\right\|_2 \le \left\|\mathbb{A}_{N_x}^{-1}\right\|_2 \left\|\mathbb{A}_{N_y}^{-1}\right\|_2 \le C$ and $\widehat{P}_k(\pm1)=(\pm1)^k$, we have

$$\begin{aligned}\Sigma_{xy} &\equiv \sum_{i=1}^{N_x}\sum_{j=1}^{N_y}\alpha_{i,j,k,k}^2 \le C\sum_{i=1}^{N_x}\sum_{j=1}^{N_y} b_{i,j,k,k}^2\\ &\le C\sum_{i=1}^{N_x}\sum_{j=1}^{N_y}\|g\|^2_{L^\infty(K_{ij})} + C\sum_{j=1}^{N_y}\sum_{l_2=0}^{k-1}\sum_{i=1}^{N_x}\alpha_{i,j,k,l_2}^2 + \sum_{i=1}^{N_x}\sum_{l_1=0}^{k-1}\sum_{j=1}^{N_y}\alpha_{i,j,l_1,k}^2\\ &\le Ch^{2\min(s,k)}\|z\|^2_{H^{s+1}(\Omega_h)},\end{aligned} \tag{3.25}$$

where the approximation properties (3.17), (3.23) and (3.24) are used.

Finally, we can obtain the approximation property by noticing the simple facts of Legendre polynomials. For example,

$$\|P_{i,l_1}(x)P_{j,l_2}(y)\|^2_{L^2(K_{i,j})} = \frac{1}{(2l_1+1)(2l_2+1)}h_i^x h_j^y \le Ch^2, \quad \forall i,j,l_1,l_2,$$

implies

$$\|E\|^2_{L^2(\Omega_h)} \le Ch^2(\Sigma_x+\Sigma_y+\Sigma_{xy}) \le Ch^{2\min(s+1,k+1)}\|z\|^2_{H^{s+1}(\Omega_h)}. \tag{3.26}$$

This completes the proof of this lemma. □

3.1.3. *Extension to the special parameter.* When the included parameters in the above projections are equal to one-half, the unique existence and approximation property become a little bit complicated. For more details, see [20, Remark 2.4].

Alternatively, we would like in this paper to define $P_{1/2}\equiv\pi_h=\pi_h^{(1\mathrm{d})}$ as one-dimensional L^2-projection rather than the global projection as in (3.2) with $\theta=1/2$, and still define P_{θ_1,θ_2} as the tensor product of one-dimensional projections, like (3.12). Namely, $P_{1/2,1/2}=\pi_h^x\otimes\pi_h^y$ is the two-dimensional L^2-projection, and

$$P_{\theta,\frac12}\equiv P_\theta^x\otimes\pi_h^y, \quad P_{\frac12,\theta}\equiv\pi_h^x\otimes P_\theta^y, \tag{3.27}$$

for $\theta\neq1/2$. Here the superscript is used to show the spatial direction of one-dimensional projection. To be more specific, for the function $z\in H^1(\Omega_h)$, the projection $P_{\theta,1/2}z\in V_h$ satisfies

$$\int_{K_{ij}}(P_{\theta,\frac12}z)v_h\mathrm{d}x\mathrm{d}y = \int_{K_{ij}} zv_h\mathrm{d}x\mathrm{d}y, \quad \forall v_h\in P^{k-1}(I_i)\otimes P^k(J_j), \tag{3.28a}$$

$$\int_{J_j}\left((P_{\theta,\frac12}z)^{\theta,y}v_h\right)_{i+\frac12,y}\mathrm{d}y = \int_{J_j}\left(z^{\theta,y}v_h\right)_{i+\frac12,y}\mathrm{d}y, \quad \forall v_h\in P^k(J_j), \tag{3.28b}$$

for any $i=1,\dots,N_x$ and $j=1,\dots,N_y$. Almost the same as above, the projection $P_{1/2,\theta}z\in V_h$ satisfies

$$\int_{K_{ij}}(P_{\frac12,\theta}z)v_h\mathrm{d}x\mathrm{d}y = \int_{K_{ij}} zv_h\mathrm{d}x\mathrm{d}y, \quad \forall v_h\in P^k(I_i)\otimes P^{k-1}(J_j), \tag{3.29a}$$

$$\int_{I_i}\left((P_{\frac12,\theta}z)^{x,\theta}v_h\right)_{x,j+\frac12}\mathrm{d}x = \int_{I_i}\left(z^{x,\theta}v_h\right)_{x,j+\frac12}\mathrm{d}x, \quad \forall v_h\in P^k(I_i) \tag{3.29b}$$

for any $i=1,\dots,N_x$ and $j=1,\dots,N_y$. This kind of global projection will be used to deal with auxiliary variables.

Lemma 3.4. *Assume $z \in H^{s+1}(\Omega_h)$ with $\Omega_h \subset \mathbb{R}^2$ and $s \geq 0$. For either $\theta_1 = 1/2$ or $\theta_2 = 1/2$, the projection $P_{\theta_1,\theta_2} z$ is well-defined and the projection error $\eta = z - P_{\theta_1,\theta_2} z$ satisfies* (3.15).

Proof. Along the same line as in Lemma 3.3, we can prove this lemma, since the circulant matrices involved in the analysis of existence are only coupled in one direction, namely in x direction for $P_{\theta_1,1/2}$ and in y direction for $P_{1/2,\theta_2}$, which is straightforward to analyze. Once existence of projections is proved, the optimal approximation properties can be easily obtained. The detailed process is omitted in this paper. □

Remark 3.5. Recalling the proofs of the above lemmas, the quasi-uniform assumption is not necessary.

3.2. **Proof for the one-dimensional case.** As usual in the finite element analysis, we denote the error by $e_u = u - u_h$ and $e_p = p - p_h$, respectively, and decompose them into two parts, namely

$$e_u = u - u_h = (u - P_\theta u) - (u_h - P_\theta u) \equiv \eta_u - \xi_u, \tag{3.30a}$$

$$e_p = p - p_h = (p - P_{\widetilde{\theta}} p) - (p_h - P_{\widetilde{\theta}} p) \equiv \eta_p - \xi_p, \tag{3.30b}$$

where the generalized Gauss–Radau projections P_θ and $P_{\widetilde{\theta}}$ have been defined in (3.2).

Due to the Sobolev embedding theory and the smooth assumption (2.25), the exact solutions u and p are continuous at every element boundary points, since $k \geq 0$. Hence, the consistence of the numerical fluxes will yield

$$\int_\Omega \frac{\partial u}{\partial t} v_h \mathrm{d}x + G_h(u, p; v_h, r_h) = 0, \quad \forall v_h, r_h \in V_h, \tag{3.31}$$

for any time $t > 0$. Subtracting (2.17) from (3.31) gives us the error equation

$$\int_\Omega \frac{\partial e_u}{\partial t} v_h \mathrm{d}x + G_h(e_u, e_p; v_h, r_h) = 0, \quad \forall v_h, r_h \in V_h. \tag{3.32}$$

Noticing the error decomposition (3.30), we have the energy identity

$$\int_\Omega \frac{\partial \xi_u}{\partial t} \xi_u \mathrm{d}x + G_h(\xi_u, \xi_p; \xi_u, \xi_p) = \int_\Omega \frac{\partial \eta_u}{\partial t} \xi_u \mathrm{d}x + G_h(\eta_u, \eta_p; \xi_u, \xi_p), \tag{3.33}$$

by taking $v_h = \xi_u$ and $r_h = \xi_p$ in (3.32).

Employing the definitions of P_θ for u and $P_{\widetilde{\theta}}$ for p, it is easy to see that

$$\int_{I_i} \eta_u \frac{\partial v_h}{\partial x} \mathrm{d}x = 0, \quad \text{and} \quad \int_{I_i} \eta_p \frac{\partial v_h}{\partial x} \mathrm{d}x = 0, \tag{3.34}$$

for any $v_h \in V_h$ in each element I_i, and $\eta_u^{(\theta)} = 0$ and $\eta_p^{(\widetilde{\theta})} = 0$ at each element boundary point. Hence,

$$H_i^{(\theta)}(\eta_u, v_h) = 0, \quad H_i^{(\widetilde{\theta})}(\eta_p, v_h) = 0, \quad \forall v_h \in V_h, \quad \forall I_i \in \Omega_h. \tag{3.35}$$

Then, using the stability result (2.22a) we can get from (3.33) that

$$\begin{aligned} \mathrm{LHS} \equiv \frac{1}{2}\frac{\mathrm{d}}{\mathrm{d}t} \|\xi_u\|^2 + \|\xi_p\|^2 + c\Big(\theta - \frac{1}{2}\Big) \sum_{i=1}^{N} [\![\xi_u]\!]_{i+\frac{1}{2}}^2 \\ = \int_\Omega \frac{\partial \eta_u}{\partial t} \xi_u \mathrm{d}x + \int_\Omega \eta_p \xi_p \mathrm{d}x \equiv \mathrm{RHS}. \end{aligned} \tag{3.36}$$

Next we estimate each term in RHS. It follows from Lemma 3.2 that

$$\left\|\frac{\partial \eta_u}{\partial t}\right\| \le Ch^{k+1}\left\|\frac{\partial u}{\partial t}\right\|_{H^{k+1}}, \quad \|\eta_p\| \le Ch^{k+1}\|p\|_{H^{k+1}},$$

since the projection is linear and independent of t. Applying Cauchy–Schwarz inequality and Young's inequality, we have

$$\begin{aligned} \text{RHS} &\le Ch^{k+1}\left\|\frac{\partial u}{\partial t}\right\|_{H^{k+1}}\|\xi_u\| + Ch^{k+1}\|p\|_{H^{k+1}}\|\xi_p\| \\ &\le Ch^{2k+2}\left[T\left\|\frac{\partial u}{\partial t}\right\|^2_{H^{k+1}} + \|p\|^2_{H^{k+1}}\right] + T^{-1}\|\xi_u\|^2 + \frac{1}{2}\|\xi_p\|^2. \end{aligned} \tag{3.37}$$

Collecting the estimates (3.36) and (3.37), and applying Gronwall's inequality, we have

$$\|\xi_u(T)\|^2 \le C\|\xi_u(0)\|^2 + Ch^{2k+2}\left[T\left\|\frac{\partial u}{\partial t}\right\|^2_{L^2(H^{k+1})} + \|p\|^2_{L^2(H^{k+1})}\right]. \tag{3.38}$$

By the setting of the initial solution, we have

$$\|\xi_u(0)\| \le \|\pi_h u_0 - u_0\| + \|u_0 - P_\theta u_0\| \le C\|u\|_{L^\infty(H^{k+1})}h^{k+1},$$

where we have used (3.5) and Lemma 3.2 for $z = u_0$. Finally, by using the triangle inequality and Lemma 3.2 again, we can complete the proof for the one-dimensional space.

3.3. **Proof for the two-dimensional case.** Along the similar line, we can prove Theorem 2.4 for the two-dimensional space. However, the proof will be much more complicated than that for the one-dimensional cases, because we have to take advantage of the superconvergence result of the generalized Gauss–Radau projection on the Cartesian meshes, and establish the following lemma.

Lemma 3.6. *Let $\theta_1 \neq \frac{1}{2}$ and $\theta_2 \neq \frac{1}{2}$. Assume $u \in H^{k+2}(\Omega_h)$, then there exists a bounding constant C independent of u, such that*

$$\left|\sum_{i=1}^{N_x}\sum_{j=1}^{N_y} H_{ij}^{l,\theta_l}\Big(u - P_{\theta_1,\theta_2}u, v_h\Big)\right| \le Ch^{k+1}\|u\|_{H^{k+2}(\Omega_h)}\|v_h\|, \tag{3.39}$$

holds on the quasi-uniform Cartesian mesh for any $v_h \in V_h$. Here H_{ij}^{l,θ_l} has been defined in subsection 2.3.1, with $l = 1, 2$.

Proof. Similar result has been discussed in [20]. However, there is a little bit improvement on the regularity requirement of the solution in current proof, so we would like to present them in details.

Since the analysis lines for different l are the same, we only give the proof for the case $l = 1$ below. The first step is to show the superconvergence result, which is almost the same as that in [20]. To be specific, it reads

$$H_{ij}^{1,\theta_1}\Big(z - P_{\theta_1,\theta_2}z, v_h\Big) = 0, \qquad \forall v_h \in Q^k(K_{ij}), \tag{3.40}$$

for any function $z \in P^{k+1}(\Omega_h)$. Here $P^{k+1}(\Omega_h)$ is the space made up of all piecewise polynomials of degree at most $k+1$ on each element.

This conclusion extends the discussion for the local Gauss–Radau projection in [10]. However, please keep in mind that the generalized Gauss–Radau projection

is defined globally, in general. That is to say, $P_{\theta_1,\theta_2}z$ may be nonzero everywhere in the whole domain, even though z is compactly supported. Thus we have to deal carefully with the influence outside of the considered element. Detailed proof can be established by the function splitting and the deep investigation on this global projection; see Appendix.

The second step is to set up the rough boundedness. In fact, using the inverse inequality [3] on the quasi-uniform Cartesian mesh for any $v_h \in Q^k(K_{ij})$,

$$\left\|\frac{\partial v_h}{\partial x}\right\|_{L^2(\Omega_h)} \le Ch^{-1}\left\|v_h\right\|_{L^2(\Omega_h)}, \quad \left\|v_h\right\|_{L^2(\Gamma_h)} \le Ch^{-\frac{1}{2}}\left\|v_h\right\|_{L^2(\Omega_h)}, \tag{3.41}$$

together with Cauchy–Schwarz inequality and Lemma 3.3, we arrive at

$$\begin{aligned}
\mathcal{LHS} \equiv & \left|\sum_{i=1}^{N_x}\sum_{j=1}^{N_y} H_{ij}^{1,\theta_1}\Big(u - P_{\theta_1,\theta_2}u, v_h\Big)\right| \\
\le & \sum_{i=1}^{N_x}\sum_{j=1}^{N_y}\left\|u - P_{\theta_1,\theta_2}u\right\|_{L^2(K_{ij})}\left\|\frac{\partial v_h}{\partial x}\right\|_{L^2(K_{ij})} \\
& + \sum_{i=1}^{N_x}\sum_{j=1}^{N_y}\left\|(u - P_{\theta_1,\theta_2}u)^{\theta_1,y}_{i+\frac{1}{2},y}\right\|_{L^2(J_j)}\left\|[\![v_h]\!]_{i+\frac{1}{2},y}\right\|_{L^2(J_j)} \\
\le & C\Big[h^{-1}\left\|u - P_{\theta_1,\theta_2}u\right\| + h^{-\frac{1}{2}}\left\|u - P_{\theta_1,\theta_2}u\right\|_{L^2(\Gamma_h)}\Big]\left\|v_h\right\| \\
\le & C\left\|u\right\|_{H^1(\Omega_h)}\left\|v_h\right\|.
\end{aligned} \tag{3.42}$$

Noticing (3.40), we will have

$$\mathcal{LHS} \le C\inf_{\chi\in P^{k+1}(\Omega_h)}\left\|u-\chi\right\|_{H^1(\Omega_h)}\left\|v_h\right\| \le Ch^{k+1}\left\|u\right\|_{H^{k+2}(\Omega_h)}\left\|v_h\right\|, \tag{3.43}$$

which completes the proof of this lemma. □

Remark 3.7. Compared with the result and analysis in [20], the main difference in this paper is that the result (3.39) is shown in the global form and the regularity assumption of u is weakened from $W^{2k+3,\infty}(\Omega_h)$ to $H^{k+2}(\Omega_h)$. This coincides with the superconvergence result (see [10, Lemma 3.6]) when the generalized Gauss–Radau projection degenerates to the local Gauss–Radau projection.

Now we are ready to establish the optimal error estimate in two-dimensional space, following the same line as before. Due to the smoothness assumption, the exact solution is continuous at every element boundary. Thus we can easily set up the error equation

$$\int_\Omega \frac{\partial e_u}{\partial t}v_h \mathrm{d}x\mathrm{d}y + G_h(e_u, e_p, e_q; v_h, r_h, s_h) = 0, \quad t > 0, \tag{3.44}$$

holding for any test function $(v_h, r_h, s_h) \in V_h \times V_h \times V_h$, where e_u, e_p and e_q are the errors with the decompositions

$$e_u = u - u_h = (u - P_{\theta_1,\theta_2}u) - (u_h - P_{\theta_1,\theta_2}u) \equiv \eta_u - \xi_u, \tag{3.45a}$$

$$e_p = p - p_h = (p - P_{\widetilde{\theta_1},\frac{1}{2}}p) - (p_h - P_{\widetilde{\theta_1},\frac{1}{2}}p) \equiv \eta_p - \xi_p, \tag{3.45b}$$

$$e_q = q - q_h = (q - P_{\frac{1}{2},\widetilde{\theta_2}}q) - (q_h - P_{\frac{1}{2},\widetilde{\theta_2}}q) \equiv \eta_q - \xi_q. \tag{3.45c}$$

Here P_{θ_1,θ_2}, $P_{\widetilde{\theta_1},1/2}$ and $P_{1/2,\widetilde{\theta_2}}$ are the generalized Gauss–Radau projections defined in (3.13), (3.28) and (3.29), respectively.

Taking the test function $v_h = \xi_u, r_h = \xi_p$ and $s_h = \xi_q$ in (3.44), and noticing the decompositions (3.45), we can arrive at the energy identity

$$\begin{aligned}\int_\Omega \frac{\partial \xi_u}{\partial t}\xi_u \mathrm{d}x\mathrm{d}y + G_h(\xi_u,\xi_p,\xi_q;\xi_u,\xi_p,\xi_q)\\ = \int_\Omega \frac{\partial \eta_u}{\partial t}\xi_u \mathrm{d}x\mathrm{d}y + G_h(\eta_u,\eta_p,\eta_q;\xi_u,\xi_p,\xi_q).\end{aligned} \tag{3.46}$$

Noticing the stability result (2.22b) and the expression of G_h, we have

$$\frac{1}{2}\frac{\mathrm{d}}{\mathrm{d}t}\left\|\xi_u\right\|^2 + \left\|\xi_p\right\|^2 + \left\|\xi_q\right\|^2 \le \mathcal{S}_1 + \mathcal{S}_2 + \mathcal{S}_3, \tag{3.47}$$

since $\theta_1 > 1/2$ and $\theta_2 > 1/2$, where

$$\begin{aligned}\mathcal{S}_1 &= \int_\Omega \frac{\partial \eta_u}{\partial t}\xi_u \mathrm{d}x\mathrm{d}y + \int_\Omega \eta_p\xi_p \mathrm{d}x\mathrm{d}y + \int_\Omega \eta_q\xi_q \mathrm{d}x\mathrm{d}y,\\ \mathcal{S}_2 &= \sum_{i=1}^{N_x}\sum_{j=1}^{N_y}\Big\{ - c_1 H_{ij}^{1,\theta_1}(\eta_u,\xi_u) + \sqrt{d_1}H_{ij}^{1,\theta_1}(\eta_u,\xi_p) + \sqrt{d_1}H_{ij}^{1,\widetilde{\theta_1}}(\eta_p,\xi_u)\Big\},\\ \mathcal{S}_3 &= \sum_{i=1}^{N_x}\sum_{j=1}^{N_y}\Big\{ - c_2 H_{ij}^{2,\theta_2}(\eta_u,\xi_u) + \sqrt{d_2}H_{ij}^{2,\theta_2}(\eta_u,\xi_q) + \sqrt{d_2}H_{ij}^{2,\widetilde{\theta_2}}(\eta_q,\xi_u)\Big\}.\end{aligned}$$

In what follows, we shall estimate them one by one.

Applying Lemmas 3.3 and 3.4, as well as Young's inequality, we obtain that

$$\begin{aligned}\mathcal{S}_1 \le T^{-1}\left\|\xi_u\right\|^2 + \frac{1}{4}\left\|\xi_p\right\|^2 + \frac{1}{4}\left\|\xi_q\right\|^2\\ + Ch^{2k+2}\left[T\left\|\frac{\partial u}{\partial t}\right\|_{H^{k+1}}^2 + \|p\|_{H^{k+1}}^2 + \|q\|_{H^{k+1}}^2\right].\end{aligned} \tag{3.48}$$

The next two terms can be estimated in a similar way, so we would like to estimate $\mathcal{S}_2$ as an example. By the definition of the projection $P_{\widetilde{\theta_1},1/2}$ (see (3.28)), it is easy to get that

$$H_{ij}^{1,\widetilde{\theta_1}}(\eta_p,\xi_u) = 0.$$

Let v_h be either ξ_u or ξ_p, both belonging to V_h. Using Lemma 3.6 we get

$$\Big|\sum_{i=1}^{N_x}\sum_{j=1}^{N_y} H_{ij}^{1,\theta_1}(\eta_u,v_h)\Big| \le Ch^{k+1}\left\|u\right\|_{H^{k+2}}\left\|v_h\right\|. \tag{3.49}$$

Hence, together with Cauchy–Schwarz inequality and Young's inequality, we obtain

$$\begin{aligned}\mathcal{S}_2 &\le Ch^{k+1}\left\|u\right\|_{H^{k+2}}\left(c_1\left\|\xi_u\right\| + \sqrt{d_1}\left\|\xi_p\right\|\right)\\ &\le T^{-1}\left\|\xi_u\right\|^2 + \frac{1}{4}\left\|\xi_p\right\|^2 + C(c^2T+d)h^{2k+2}\left\|u\right\|_{H^{k+2}}^2,\end{aligned} \tag{3.50}$$

where $c = \max(c_1,c_2)$ and $d = \max(d_1,d_2)$. Analogously, we have

$$\mathcal{S}_3 \le T^{-1}\left\|\xi_u\right\|^2 + \frac{1}{4}\left\|\xi_q\right\|^2 + C(c^2T+d)h^{2k+2}\left\|u\right\|_{H^{k+2}}^2. \tag{3.51}$$

Finally, inserting (3.48), (3.50) and (3.51) into (3.47), and applying Gronwall's inequality, we arrive at

$$\|\xi_u(T)\|^2 \le C\,\|\xi_u(0)\|^2 + C(1+T)h^{2k+2}\Big[\,\|u\|^2_{L^2(H^{k+2})} + \|u_t\|^2_{L^2(H^{k+1})}\,\Big].$$

By the setting of the initial solution and the triangle inequality, we can complete the proof of this theorem for the two-dimensional space.

3.4. **Error estimates when the special parameters are used.** At the end of this section we give a supplement remark, when the parameter in the numerical fluxes (2.8) or (2.16) is taken to be 1/2. This setting is acceptable in the semi-discrete LDG method, although it is not a good choice in the fully discrete LDG method, for example, the explicit time-marching when solving the convection-dominated diffusion equations. It is well known for this situation that the optimal convergence order is also observed numerically in the uniform mesh when the degree of polynomials k is even, no matter the element number in one direction is even or odd. How to prove this numerical behavior in theory is an interesting issue.

Let us start from the one-dimensional case. At this moment, we will encounter some trouble by using the original definition of generalized Gauss-Radau projection, namely letting $\theta = 1/2$ in (3.2). For even k, the unique existence of this projection holds only for odd N; see (3.8). Furthermore, we can obtain the optimal approximation property by virtue of the super-convergence resulting from the uniform mesh for sufficiently smooth functions. The detailed analysis is complex and lengthy. For more details, we refer the readers to [20, Remark 2.4], and [2, Proposition 3.2].

However, the proof can be simplified by using the the local L^2-projection $\pi_h^{(1\mathrm{d})}$, which is defined in this paper as $P_{1/2}$ for the uniform of notations; see subsection 3.1.3 for details. To show that, let us give a sketch of the proof. Repeating the process as in subsection 3.2, we will find out that (3.35) is not true, since the errors at element boundaries cannot be eliminated completely, when the local L^2-projection, (2.6), is used. As a result, the right-hand side in (3.36) is changed to

$$\mathrm{RHS} = -c\sum_{i=1}^{N}(\eta_u)^{(\frac12)}_{i+\frac12}[\![\xi_u]\!]_{i+\frac12} + \sqrt{d}\sum_{i=1}^{N}(\eta_p)^{(\frac12)}_{i+\frac12}[\![\xi_u]\!]_{i+\frac12} + \sqrt{d}\sum_{i=1}^{N}(\eta_u)^{(\frac12)}_{i+\frac12}[\![\xi_p]\!]_{i+\frac12},$$

where $\eta_z = z - \pi_h^{(1\mathrm{d})}z$ for $z = u, p$. It is well known that, for general k and quasi-uniform mesh, only suboptimal convergence result of order k can be proved, due to the application of inverse inequality. However, if k is even and the mesh is uniform, there holds the superconvergence property [13, Lemma 2.5]

$$|(\eta_z)^{(\frac12)}_{i+\frac12}| \le Ch^{k+\frac32}\,\|z\|_{H^{k+2}(I_i\cup I_{i+1})}, \quad i = 1, \cdots, N. \tag{3.52}$$

Taking into account the inverse property and the Young's inequality, we will obtain

$$\frac12\frac{\mathrm{d}}{\mathrm{d}t}\,\|\xi_u\|^2 + \frac12\,\|\xi_p\|^2 \le C\Big[\,\|\xi_u\|^2 + h^{2k+2}\Big]. \tag{3.53}$$

Application of Gronwall's inequality leads to the optimal error estimate in the L^2 norm.

Discussion for the two-dimensional case is similar when k is even and the Cartesian mesh is uniform in the direction in which the corresponding parameter is equal to 1/2. In whatever case, we can obtain the optimal error estimate along the same

line as before, by using the projection P_{θ_1,θ_2}, as we have mentioned in subsection 3.1.3, and establishing the approximation property (Lemma 3.4) and the superconvergence property similar to Lemma 3.6. The process is almost the same and lengthy, so we omit them to save space.

4. Different parameters for convection and diffusion parts

In this section we are going to extend the previous analysis to the LDG method with more general numerical fluxes in which the parameters about the prime variable u_h emerging from the convection part and the diffusion part are independently chosen. For example, we can consider

$$(\hat{h}_u, \hat{h}_p) = (cu_h^{(\theta)} - \sqrt{d}p_h^{(\widetilde{\gamma})}, -\sqrt{d}u_h^{(\gamma)}) \tag{4.1}$$

for one-dimensional space, and

$$(\hat{h}_{1u}, \hat{h}_p) = \Big(c_1 u_h^{\theta_1,y} - \sqrt{d}p_h^{\widetilde{\gamma_1},y}, -\sqrt{d}u_h^{\gamma_1,y}\Big), \tag{4.2a}$$

$$(\hat{h}_{2u}, \hat{h}_q) = \Big(c_2 u_h^{x,\theta_2} - \sqrt{d}q_h^{x,\widetilde{\gamma_2}}, -\sqrt{d}u_h^{x,\gamma_2}\Big), \tag{4.2b}$$

for two-dimensional space. Note that the identities in (2.22) also hold for the LDG methods when the general numerical fluxes are used. Hence the stability results stated in Theorem 2.3 also hold.

Below we will focus our attention on the error estimates in L^2-norm. To save space, we would like to take the one-dimensional case as an example. However, we will point out the main differences for two-dimensional case at the end of this section; see Remark 4.1.

Assume $\theta \neq \frac{1}{2}$ and $\gamma \neq \frac{1}{2}$ for simplicity. Let us recall the proof in subsection 3.2, and keep in mind that the error equation (3.33) still holds, with the main term

$$\begin{aligned} G_h(\eta_u, \eta_p; \xi_u, \xi_p) &= \int_\Omega \eta_p \xi_p \mathrm{d}x \\ &\quad + \sum_{i=1}^{N} \Big\{ -cH_i^{(\theta)}(\eta_u, \xi_u) + \sqrt{d}H_i^{(\widetilde{\gamma})}(\eta_p, \xi_u) + \sqrt{d}H_i^{(\gamma)}(\eta_u, \xi_p) \Big\}, \end{aligned} \tag{4.3}$$

where ξ_u, ξ_p, η_u and η_p may be in different definition in each occurrence depending on the choice of projections.

4.1. **Direct applications.** In general, we cannot obtain the optimal error estimate, if $\gamma \neq \theta$, by directly using the current approach, because we are no longer able to introduce a specific generalized Gauss–Radau projection to eliminate simultaneously those errors on the element boundaries and in particular for the prime variable u emerging from the convection part and the diffusion part.

For example, if we want to eliminate completely the boundary errors coming from the diffusion part, we can define

$$\eta_u = u - P_\gamma u \quad \text{and} \quad \eta_p = p - P_{\widetilde{\gamma}} p, \tag{4.4}$$

where P_γ and $P_{\widetilde{\gamma}}$ have already been constructed before. It is easy to see that (3.34) holds for any $v_h \in V_h$ in each element, and that $\eta_u^{(\gamma)} = 0$ and $\eta_p^{(\tilde{\gamma})} = 0$ hold at each element boundary point. However, in general

$$\eta_u^{(\theta)} = \eta_u^{(\gamma)} + (\gamma - \theta)[\![\eta_u]\!] = (\gamma - \theta)[\![\eta_u]\!] \neq 0,$$

if $\gamma \neq \theta$. Therefore, some boundary terms about the projection error are left, so that a new term $\sum_{i=1}^{n} c(\theta-\gamma)([\![\eta_u]\!][\![\xi_u]\!])_{i+\frac{1}{2}}$ is supplemented on the right-hand side of (3.36). Using Young's inequality, we can bound this term by the numerical stability (the boundary term in (3.36)) and the approximation property in Lemma 3.2. Along the same line as before, we can obtain the error estimate

$$\|u(T)-u_h(T)\| \leq C(1+T)\Big[h^{k+1}+\sqrt{c}|\gamma-\theta|h^{k+\frac{1}{2}}\Big], \tag{4.5}$$

under the same regularity assumption as that in Theorem 2.4, and $d \geq 0$.

On the other hand, if we want to eliminate completely the boundary errors coming from the convection part, we can define

$$\eta_u = u - P_\theta u \quad \text{and} \quad \eta_p = p - P_{\widetilde{\theta}} p.$$

Along the same analysis as before, we can easily see that a new term $\sum_{i=1}^{N}\sqrt{d}(\gamma-\theta)([\![\eta_p]\!][\![\xi_u]\!]-[\![\eta_u]\!][\![\xi_p]\!])_{i+\frac{1}{2}}$ is added to the right-hand side of (3.36), which can be bounded by the numerical stability and the approximation property, with the help of Young's inequality and the inverse inequality on the quasi-uniform mesh

$$\sum_{i=1}^{N}[\![\xi_p]\!]_{i+\frac{1}{2}}^2 \leq Ch^{-1}\left\|\xi_p\right\|^2.$$

Next, an application of Cauchy–Schwarz inequality and Gronwall's inequality yields the error estimate

$$\|u(T)-u_h(T)\| \leq C(1+T)\left[h^{k+1}+\sqrt{d}|\gamma-\theta|h^{k}\right], \tag{4.6}$$

under the same regularity assumption as that in Theorem 2.4, and $d \geq 0$.

4.2. **A new projection.** It is well-known that the optimal convergence order is often observed in numerical experiments if $d > 0$. To prove this in theory, we have to find a new approach to completely eliminate the projection errors on element boundaries.

Slightly motivated by [8], in which the projection is adopted to be a suitable combination of the prime variable and the auxiliary variable, we would like to define for any vector-valued function $z = (z_u, z_p) \in C(\bar{\Omega}_h) \times C(\bar{\Omega}_h)$ a new projection

$$\Pi_h(z_u, z_p) = (P_\gamma z_u, P^\star_{\widetilde{\gamma}} z_p), \tag{4.7}$$

in which $P_\gamma z_u \in V_h$ is defined as that in (3.2), and $P^\star_{\widetilde{\gamma}} z_p \in V_h$ depends on both z_p and z_u, such that

$$\int_{I_i}(P^\star_{\widetilde{\gamma}} z_p)v_h \mathrm{d}x = \int_{I_i} z_p v_h \mathrm{d}x, \quad \forall v_h \in P^{k-1}(I_i), \tag{4.8a}$$

$$(P^\star_{\widetilde{\gamma}} z_p)^{(\widetilde{\gamma})}_{i+\frac{1}{2}} = (z_p^{(\widetilde{\gamma})})_{i+\frac{1}{2}} - \frac{c}{\sqrt{d}}(\gamma-\theta)[\![z_u - P_\gamma z_u]\!]_{i+\frac{1}{2}}, \tag{4.8b}$$

for any $i = 1, \ldots, N$. Note that $P^\star_{\widetilde{\gamma}} z_p = P_{\widetilde{\gamma}} z_p$ if $\gamma = \theta$. It is easy to see that $P_\gamma z_u = z_u$ and $P^\star_{\widetilde{\gamma}} z_p = z_p$, if z_u and z_p both belong to V_h. Hence Π_h is indeed a projection.

By using an analysis similar to that in [20] and in Lemma 3.2, we can derive the unique existence of this projection and the approximation property

$$\left\|z_p - P^\star_{\widetilde{\gamma}} z_p\right\| \leq Ch^{k+1}\left(\|z_p\|_{H^{k+1}(\Omega_h)} + \frac{c}{\sqrt{d}}|\gamma-\theta|\cdot\|z_u\|_{H^{k+1}(\Omega_h)}\right), \tag{4.9}$$

since $z_u - P_\gamma z_u$ is already known to be of order h^{k+1}, due to Lemma 3.2.

To derive the error estimate, let us revisit the energy identity (3.33), with

$$\eta_u = u - P_\gamma u, \quad \eta_p = p - P^\star_{\widetilde{\gamma}} p, \tag{4.10}$$

By using the definition of projection Π_h, we can also obtain (3.34) for any $v_h \in V_h$ in each element, and find out

$$\eta_u^{(\gamma)} = 0, \quad \eta_p^{(\widetilde{\gamma})} = \frac{c}{\sqrt{d}}(\gamma - \theta)[\![\eta_u]\!] \tag{4.11}$$

at every element boundary point. Hence we can have that $H_i^{(\gamma)}(\eta_u, v_h) = 0$ holds for any $v_h \in V_h$ and

$$\begin{aligned} &\sum_{i=1}^{N} \left(-cH_i^{(\theta)}(\eta_u, \xi_u) + \sqrt{d} H_i^{(\widetilde{\gamma})}(\eta_p, \xi_u) \right) \\ &\qquad = \sum_{i=1}^{N} \left(-c\eta_u^{(\theta)} + \sqrt{d}\eta_p^{(\widetilde{\gamma})} \right)_{i+\frac{1}{2}} [\![\xi_u]\!]_{i+\frac{1}{2}} = 0, \end{aligned} \tag{4.12}$$

due to the simple fact that $\eta_u^{(\theta)} = (\gamma - \theta)[\![\eta_u]\!]$. One is excited to see that all the projection errors at the element boundaries are completely eliminated. Hence

$$G_h(\eta_u, \eta_p; \xi_u, \xi_p) = \int_\Omega \eta_p \xi_p \mathrm{d}x,$$

and the inequality (3.36) also holds. Repeating the similar arguments as before, we can use Gronwall's inequality to obtain the optimal error estimate

$$\|u(T) - u_h(T)\| \le C(1+T)\left(1 + \frac{c}{\sqrt{d}}|\gamma - \theta|\right) h^{k+1}, \tag{4.13}$$

under the same regularity assumption as that in Theorem 2.4.

4.3. **A unified estimate.** Finally, we collect the above three estimates, i.e. (4.5), (4.6) and (4.13) to get the following unified result

$$\|u(T) - u_h(T)\| \le C(1+T)\Big[h^{k+1} + \sqrt{c}\min\Big(\frac{\sqrt{ch}}{\sqrt{d}}, \frac{\sqrt{d}}{\sqrt{ch}}, 1\Big)|\gamma - \theta| h^{k+\frac{1}{2}}\Big], \tag{4.14}$$

where the bounding constant C is independent of h and d^{-1}. This result holds robustly for whatever the problem is convection-dominated or not.

Obviously, the result (4.14) coincides with Theorem 2.4 when $\theta = \gamma$. Otherwise, if $\gamma \neq \theta$, the mesh Péclet number ch/d will play an important role. Namely,

$$\|u(T) - u_h(T)\| = \begin{cases} \mathcal{O}(h^{k+1}), & d/(ch) \ge \mathcal{O}(h^{-1}) \quad \text{or} \quad d/(ch) \le \mathcal{O}(h), \\ \mathcal{O}(h^{k+1/2}), & d/(ch) \approx \mathcal{O}(1). \end{cases}$$

There is a little reduction on the error order in the case $d \approx ch$. Hence, we suggest using the same parameters in the numerical fluxes to get the best robustness in the accuracy.

Remark 4.1. The above analysis can be easily extended to multi-dimensional cases. For example, assuming $\gamma_1 \neq 1/2$ and $\gamma_2 \neq 1/2$ for two-dimensional case, we define for any vector-valued function $z = (z_u, z_p, z_q) \in C(\bar{\Omega}_h) \times C(\bar{\Omega}_h) \times C(\bar{\Omega}_h)$ a new projection

$$\Pi_h^{(2\mathrm{d})}(z_u, z_p, z_q) = (P_{\gamma_1,\gamma_2} z_u, P^\star_{\widetilde{\gamma_1},\frac{1}{2}} z_p, P^\star_{\frac{1}{2},\widetilde{\gamma_2}} z_q), \tag{4.15}$$

in which $P_{\gamma_1,\gamma_2} z_u \in V_h$ is defined as that in (3.13), and $P^\star_{\widehat{\gamma_1},1/2} z_p$ is defined as the unique element in V_h such that

(4.16a)
$$\int_{K_{ij}} (z_p - P^\star_{\widehat{\gamma_1},\frac{1}{2}} z_p) v_h \mathrm{d}x\mathrm{d}y = 0, \quad \forall v_h \in P^{k-1}(I_i) \otimes P^k(J_j),$$

(4.16b)
$$\int_{J_j} \left((z_p - P^\star_{\widehat{\gamma_1},\frac{1}{2}} z_p)^{\widehat{\gamma_1},y} v_h \right)_{i+\frac{1}{2},y} \mathrm{d}y = \frac{c_1}{\sqrt{d_1}} (\gamma_1 - \theta_1) \int_{J_j} \left([\![z_u - P_{\gamma_1,\gamma_2} z_u]\!] v_h \right)_{i+\frac{1}{2},y} \mathrm{d}y, \quad \forall v_h \in P^k(J_j),$$

hold for any $i = 1, \ldots, N_x$ and $j = 1, \ldots, N_y$. Note that $P^\star_{1/2,\widehat{\gamma_2}} z_q$ can be defined in a similar way, so omitted here. Obviously, $\Pi_h^{(2\mathrm{d})}$ is indeed a projection.

Using the above new projection and defining

$$\eta_u = u - P_{\gamma_1,\gamma_2} u, \quad \eta_p = p - P^\star_{\widehat{\gamma_1},\frac{1}{2}} p, \quad \eta_q = q - P^\star_{\frac{1}{2},\widehat{\gamma_2}} q,$$

we can repeat the above analysis to obtain the optimal error estimate, since the super-convergence property stated in Lemma 3.6 still holds. We will, however, omit the details to save space.

5. Numerical experiments

The purpose of this section is to numerically validate the optimal a priori error estimates of the LDG method using generalized alternating numerical fluxes for the linear convection-diffusion equation.

5.1. **Example 1.** Consider (1.1) in the domain $(0, 2\pi)^m \times [0, T]$ with the periodic boundary condition. Let the exact solution be

$$u(x_1, \ldots, x_m, t) = \exp\left(-\sum_{\ell=1}^m d_\ell t \right) \sin\left(\sum_{\ell=1}^m x_\ell - \sum_{\ell=1}^m c_\ell t \right), \quad m = 1, 2, \tag{5.1}$$

where the parameters are listed as follows

(5.2)

	c	d	T	c_1	c_2	d_1	d_2	T
Test A:	1	10^{-5}	1	1	1	10^{-5}	10^{-5}	0.1
Test B:	1	1	1	1	1	1	1	0.1
Test C:	0	1	1	0	0	1	1	0.1

The initial solution and the source term f can be determined by this solution.

We will carry out the LDG method with the piecewise polynomials of degree at most k in each variable. For all the cases, we use the strong stability preserving (SSP) ninth-order time discretization [17] with small time step, such that the overall error is dominated by the spatial error. Moreover, we divide the space into N^m-elements to form the uniform mesh, and then randomly perturb the coordinates of horizontal lines and vertical line by 10% to construct the nonuniform mesh. The convergence order in this paper is computed by

$$\mathrm{order}_N = \left[\log(\mathrm{error}_{N/2}) - \log(\mathrm{error}_N) \right] / \log 2,$$

where error_N represents the L^2-norm error at the final time T when the total number of used mesh is equal to N^m.

We firstly investigate the one-dimensional LDG scheme with the numerical flux (2.8), where θ is $0.75, 1.0$ and 2.0, respectively. Tables 5.1 and 5.2 show the optimal convergence orders for both the uniform and nonuniform meshes, when the parameters for the primal variable on the convection and diffusion parts in the numerical fluxes are the same. This coincides with Theorem 2.4 and shows the sharpness of theoretical results.

For the two-dimensional LDG scheme with the numerical flux (2.16), with different combinations of θ_1 and θ_2, we also investigate the numerical performance. Figures 5.1–5.3 show the convergence orders for three examples, where the logarithm of L^2 errors are plotted for refining meshes, with the total number of elements being $10^2, 20^2, 40^2$ and 80^2, respectively. In each figure, both the uniform mesh and nonuniform mesh, as well as different combinations of θ_1 and θ_2 are considered. The optimal convergence orders in these figures show that the result in Theorem 2.4 is sharp.

5.2. **Example 2.** Let us continue to consider the same problem in Example 1, and investigate the numerical behaviors when the including parameters are not the same.

To this end, we take $\theta = 0.75$ and let γ be valued $1.0, 1.5$ and 2.0, respectively, in the one-dimensional LDG scheme with the numerical flux (4.1). We can see from table 5.3 that, there are only little difference for the errors no matter two parameters are equal to or not, or the mesh is uniform or not. The optimal convergence orders are also observed numerically, which coincides with theoretical results obtained in section 4.

As for the two-dimensional problem, similar numerical results can be observed. We omit them to save space.

5.3. **Example 3.** To investigate the optimality of the smoothness on the exact solution given by Theorem 2.4, let us consider (1.1) in one-dimensional space with $c = d = 1$, together with the exact solution

$$u(x,t) = [\sin(x-t)]^{2.6}. \tag{5.3}$$

We implement the LDG method with $\theta = 0.75$ in (2.8) on the uniform mesh and nonuniform mesh, respectively, till $T = 1$. The numerical errors and convergence orders are listed in Table 5.4. Since the function in (5.3) does not belong to $L^\infty(H^3) \cap L^2(H^4)$, the optimal convergence order is not observed for P^2 and P^3 finite elements, as Theorem 2.4 predicts. It shows that the smoothness assumptions on the exact solution (2.25) are reasonable.

6. Concluding remarks

In this paper, we obtain the optimal L^2-norm error estimates for the LDG method by using generalized alternating numerical fluxes, when solving the linear convection-diffusion problems. The main technique is the construction and analysis of the generalized Gauss–Radau projections and its extensions, which is successful in getting rid of the dual argument.

In the further work, we will consider other kinds of boundary conditions, the variable-coefficient linear equations and even the degenerate diffusion problems.

			$\theta = 0.75$		$\theta = 1.0$		$\theta = 2.0$	
		N	error	order	error	order	error	order
A	P^0	20	2.10E-01	-	3.02E-01	-	6.79E-01	-
		40	1.06E-01	0.99	1.56E-01	0.95	3.80E-01	0.84
		80	5.30E-02	0.99	7.92E-02	0.98	2.01E-01	0.92
		160	2.66E-02	1.00	3.99E-02	0.99	1.03E-01	0.96
	P^1	20	1.69E-02	-	1.06E-02	-	7.24E-03	-
		40	4.45E-03	1.93	2.67E-03	1.99	1.80E-03	2.01
		80	1.13E-03	1.98	6.69E-04	2.00	4.49E-04	2.00
		160	2.83E-04	2.00	1.67E-04	2.00	1.12E-04	2.00
	P^2	20	2.09E-04	-	2.74E-04	-	5.74E-04	-
		40	2.59E-05	3.01	3.42E-05	3.00	7.85E-05	2.87
		80	3.23E-06	3.00	4.28E-06	3.00	1.00E-05	2.96
		160	4.04E-07	3.00	5.35E-07	3.00	1.26E-06	2.99
	P^3	20	8.44E-06	-	5.42E-06	-	3.94E-06	-
		40	5.46E-07	3.95	3.43E-07	3.98	2.49E-07	3.99
		80	3.44E-08	3.99	2.12E-08	4.01	1.52E-08	4.03
		160	2.15E-09	4.00	1.33E-09	4.00	9.53E-10	3.99
B	P^0	20	6.84E-02	-	1.07E-01	-	3.17E-01	-
		40	3.63E-02	0.91	5.63E-02	0.93	1.63E-01	0.96
		80	1.88E-02	0.95	2.89E-02	0.96	8.06E-02	1.02
		160	9.60E-03	0.97	1.46E-02	0.98	3.98E-02	1.02
	P^1	20	6.43E-03	-	3.95E-03	-	2.67E-03	-
		40	1.65E-03	1.96	9.86E-04	2.00	6.62E-04	2.01
		80	4.16E-04	1.99	2.46E-04	2.00	1.65E-04	2.00
		160	1.04E-04	2.00	6.16E-05	2.00	4.12E-05	2.00
	P^2	20	7.68E-05	-	1.01E-04	-	2.14E-04	-
		40	9.53E-06	3.01	1.26E-05	3.00	2.89E-05	2.89
		80	1.19E-06	3.00	1.57E-06	3.00	3.69E-06	2.97
		160	1.49E-07	3.00	1.97E-07	3.00	4.64E-07	2.99
	P^3	20	3.12E-06	-	2.00E-06	-	1.45E-06	-
		40	2.01E-07	3.96	1.25E-07	4.00	9.00E-08	4.01
		80	1.27E-08	3.99	7.82E-09	4.00	5.61E-09	4.00
		160	7.93E-10	4.00	4.89E-10	4.00	3.51E-10	4.00
C	P^0	20	6.17E-02	-	5.94E-02	-	1.25E-01	-
		40	2.99E-02	1.04	2.97E-02	1.00	4.21E-02	1.57
		80	1.49E-02	1.01	1.48E-02	1.00	1.67E-02	1.34
		160	7.42E-03	1.00	7.41E-03	1.00	7.66E-03	1.12
	P^1	20	6.38E-03	-	3.95E-03	-	2.67E-03	-
		40	1.65E-03	1.95	9.86E-04	2.00	6.62E-04	2.01
		80	4.15E-04	1.99	2.46E-04	2.00	1.65E-04	2.00
		160	1.04E-04	2.00	6.16E-05	2.00	4.12E-05	2.00
	P^2	20	7.68E-05	-	1.01E-04	-	2.13E-04	-
		40	9.54E-06	3.01	1.26E-05	3.00	2.89E-05	2.88
		80	1.19E-06	3.00	1.57E-06	3.00	3.69E-06	2.97
		160	1.49E-07	3.00	1.97E-07	3.00	4.64E-07	2.99
	P^3	20	3.12E-06	-	2.00E-06	-	1.45E-06	-
		40	2.01E-07	3.96	1.25E-07	4.00	9.00E-08	4.01
		80	1.27E-08	3.99	7.82E-09	4.00	5.61E-09	4.00
		160	7.93E-10	4.00	4.89E-10	4.00	3.51E-10	4.00

TABLE 5.1. L^2-norm errors and convergence orders on one-dimensional uniform meshes.

			$\theta = 0.75$		$\theta = 1.0$		$\theta = 2.0$	
		N	error	order	error	order	error	order
A	P^0	20	2.13E-01	-	3.07E-01	-	6.75E-01	-
		40	1.08E-01	0.97	1.58E-01	0.96	3.80E-01	0.83
		80	5.45E-02	0.99	7.98E-02	0.98	2.01E-01	0.92
		160	2.74E-02	0.99	4.03E-02	0.99	1.04E-01	0.96
	P^1	20	1.78E-02	-	1.07E-02	-	7.65E-03	-
		40	4.48E-03	1.99	2.75E-03	1.96	1.98E-03	1.95
		80	1.15E-03	1.96	6.97E-04	1.98	4.80E-04	2.04
		160	2.87E-04	2.00	1.72E-04	2.02	1.23E-04	1.97
	P^2	20	2.31E-04	-	3.00E-04	-	5.92E-04	-
		40	3.05E-05	2.92	3.73E-05	3.01	8.21E-05	2.85
		80	3.71E-06	3.04	4.55E-06	3.04	1.03E-05	3.00
		160	4.54E-07	3.03	5.74E-07	2.98	1.30E-06	2.98
	P^3	20	9.41E-06	-	5.95E-06	-	4.46E-06	-
		40	5.81E-07	4.02	3.75E-07	3.99	3.51E-07	3.67
		80	3.66E-08	3.99	2.45E-08	3.94	1.95E-08	4.17
		160	2.28E-09	4.00	1.47E-09	4.06	1.35E-09	3.85
B	P^0	20	7.09E-02	-	1.10E-01	-	3.21E-01	-
		40	3.70E-02	0.94	5.68E-02	0.95	1.63E-01	0.98
		80	1.92E-02	0.95	2.91E-02	0.97	8.06E-02	1.02
		160	9.80E-03	0.97	1.47E-02	0.98	3.98E-02	1.02
	P^1	20	6.55E-03	-	4.08E-03	-	2.90E-03	-
		40	1.69E-03	1.96	1.03E-03	1.99	7.27E-04	2.00
		80	4.21E-04	2.00	2.53E-04	2.02	1.79E-04	2.02
		160	1.05E-04	2.00	6.31E-05	2.00	4.47E-05	2.00
	P^2	20	8.69E-05	-	1.07E-04	-	2.26E-04	-
		40	1.04E-05	3.06	1.32E-05	3.02	2.97E-05	2.92
		80	1.33E-06	2.98	1.67E-06	2.98	3.77E-06	2.98
		160	1.65E-07	3.00	2.09E-07	3.00	4.74E-07	2.99
	P^3	20	3.18E-06	-	2.14E-06	-	1.81E-06	-
		40	2.13E-07	3.90	1.38E-07	3.96	1.12E-07	4.01
		80	1.35E-08	3.98	8.68E-09	3.99	7.10E-09	3.97
		160	8.42E-10	4.00	5.39E-10	4.01	4.40E-10	4.01
C	P^0	20	6.23E-02	-	6.20E-02	-	1.27E-01	-
		40	3.07E-02	1.02	3.02E-02	1.04	4.28E-02	1.57
		80	1.53E-02	1.00	1.51E-02	1.00	1.69E-02	1.34
		160	7.59E-03	1.01	7.55E-03	1.00	7.80E-03	1.11
	P^1	20	6.55E-03	-	4.08E-03	-	2.90E-03	-
		40	1.70E-03	1.96	1.03E-03	1.99	7.27E-04	2.00
		80	4.21E-04	2.00	2.53E-04	2.02	1.79E-04	2.02
		160	1.05E-04	2.00	6.31E-05	2.00	4.47E-05	2.00
	P^2	20	8.82E-05	-	1.10E-04	-	2.26E-04	-
		40	1.08E-05	3.02	1.35E-05	3.02	2.97E-05	2.92
		80	1.31E-06	3.04	1.66E-06	3.03	3.77E-06	2.98
		160	1.64E-07	3.00	2.07E-07	3.00	4.74E-07	2.99
	P^3	20	3.18E-06	-	2.14E-06	-	1.81E-06	-
		40	2.13E-07	3.90	1.38E-07	3.96	1.12E-07	4.01
		80	1.35E-08	3.98	8.68E-09	3.99	7.10E-09	3.97
		160	8.42E-010	4.00	5.39E-010	4.01	4.40E-010	4.01

TABLE 5.2. L^2-norm errors and convergence orders on one-dimensional nonuniform meshes.

FIGURE 5.1. L^2-norm convergence orders for Test A on two-dimensional uniform mesh (left column) and nonuniform mesh (right column).

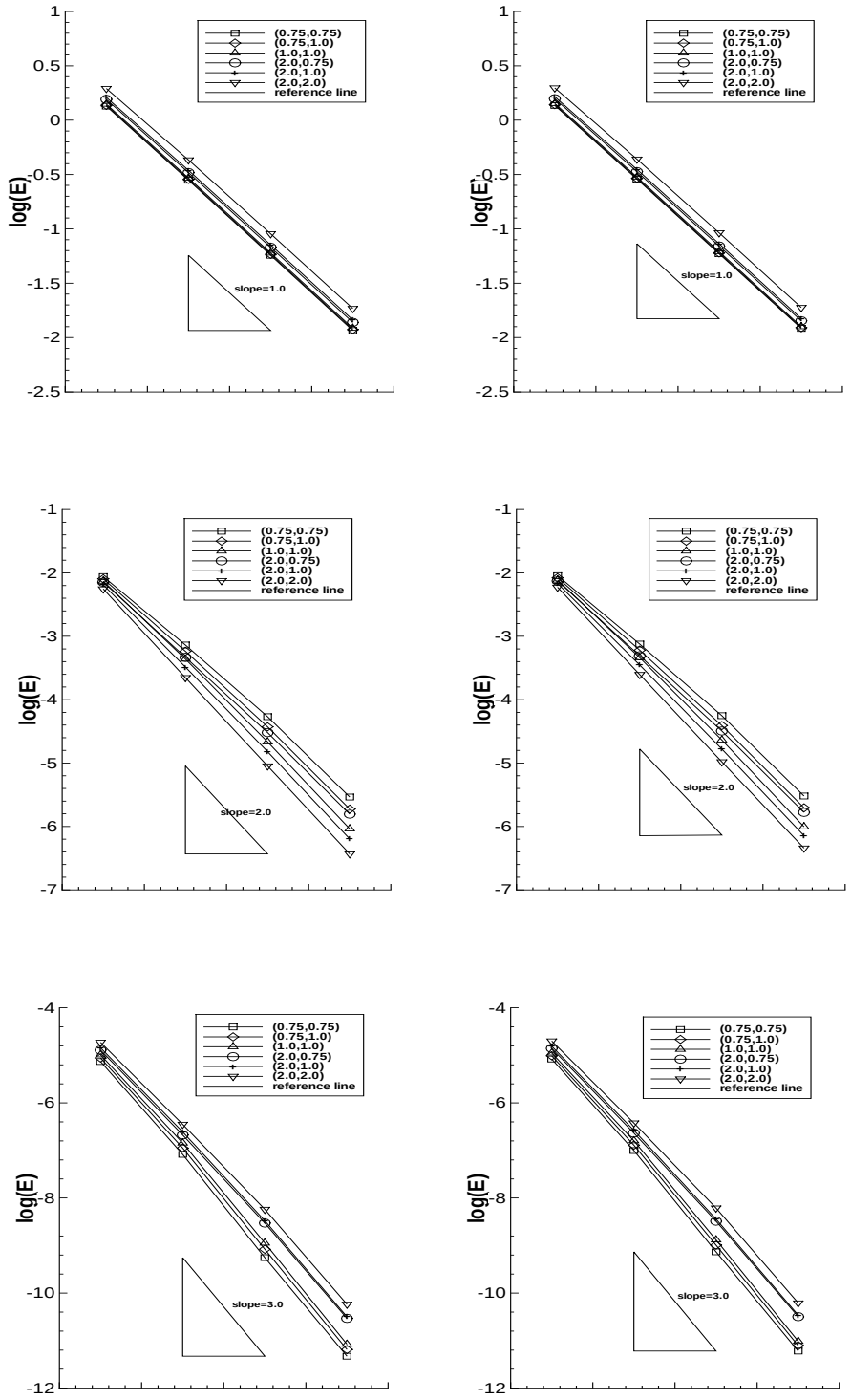

FIGURE 5.2. L^2-norm convergence orders for Test B on two-dimensional uniform mesh (left column) and nonuniform mesh (right column).

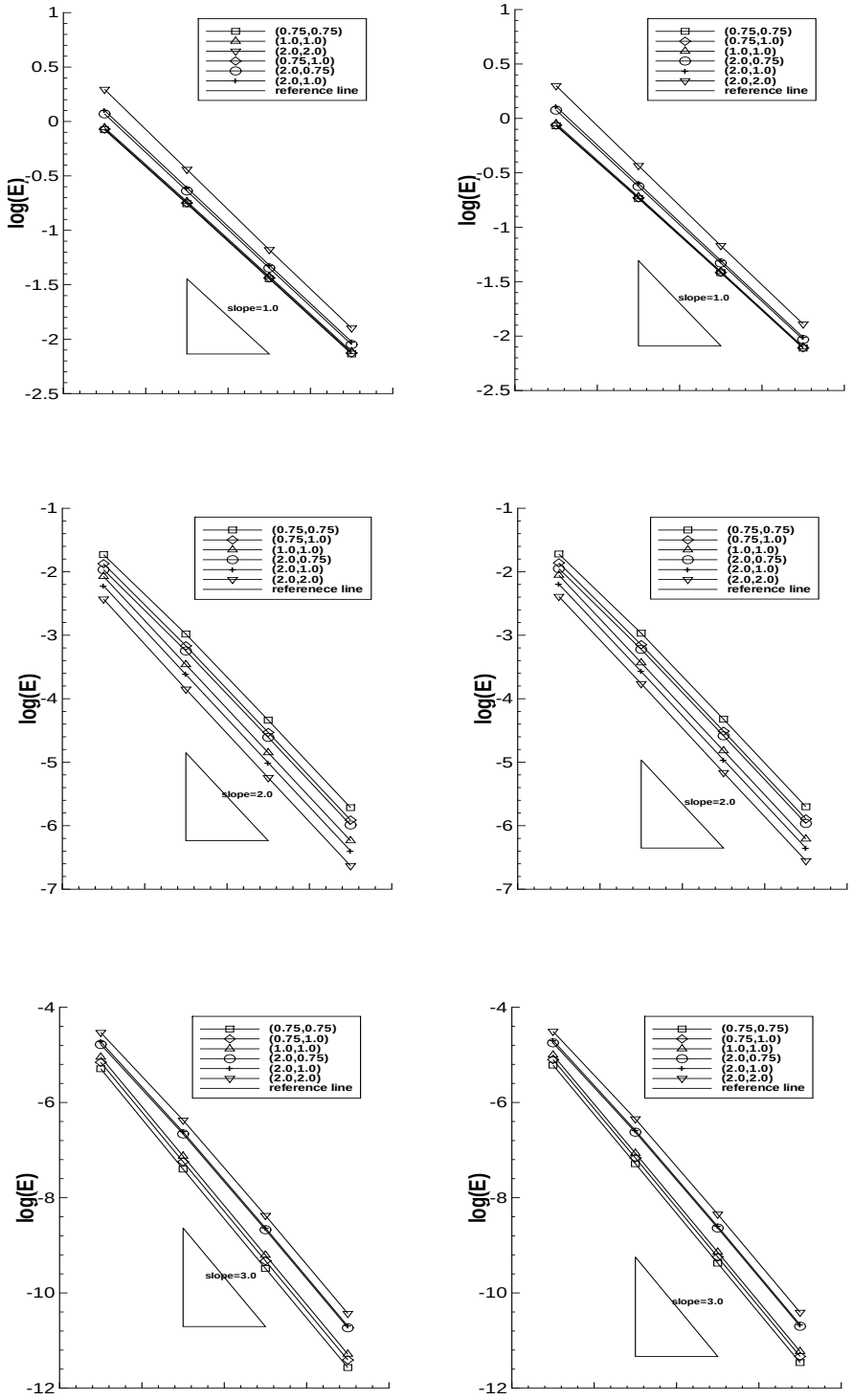

FIGURE 5.3. L^2-norm convergence orders for Test C on two-dimensional uniform mesh (left column) and nonuniform mesh (right column).

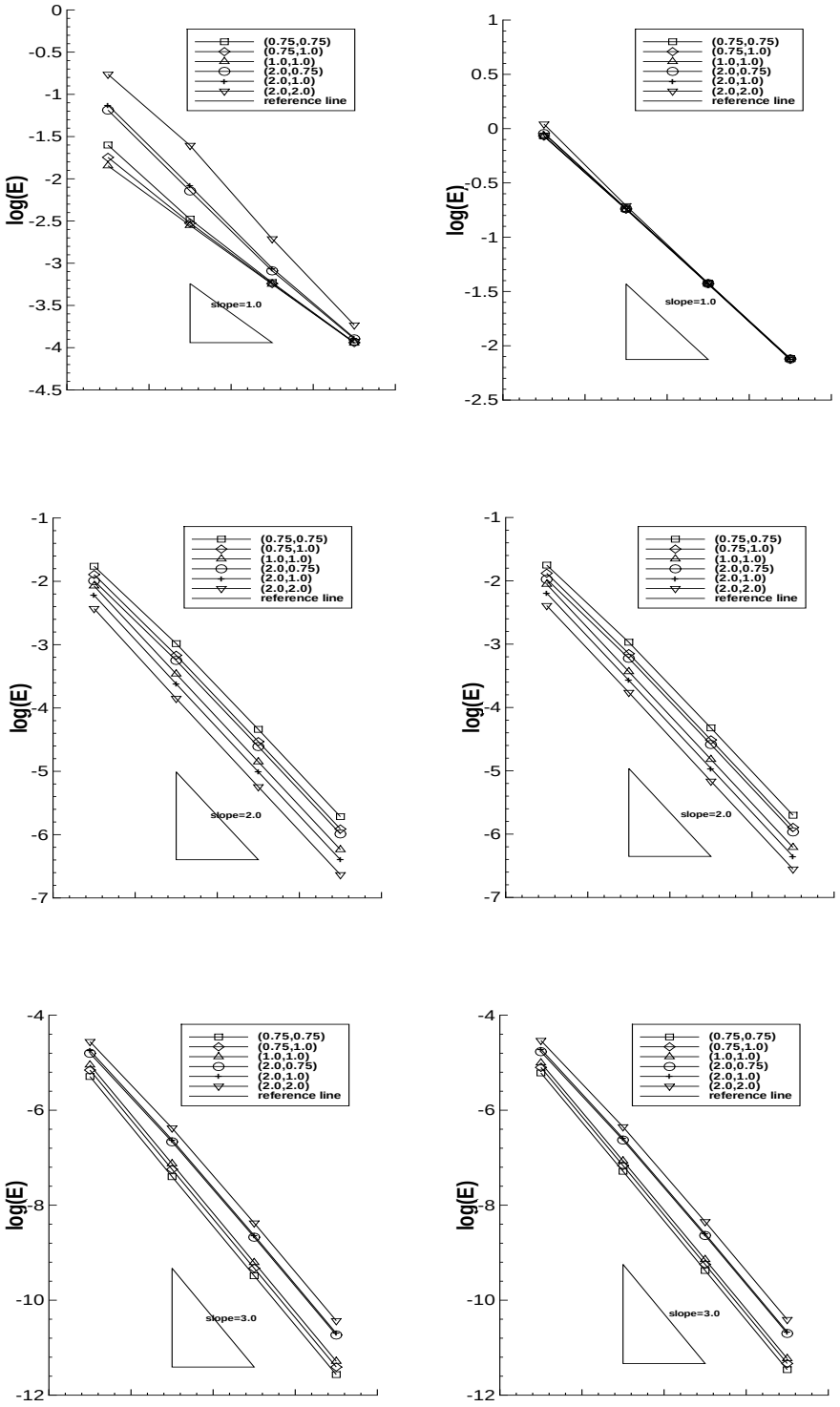

(a) uniform meshes

			$\gamma = 1.0$		$\gamma = 1.5$		$\gamma = 2.0$	
		N	error	order	error	order	error	order
A	P^1	20	1.69E-02	-	1.69E-02	-	1.69E-02	-
		40	4.45E-03	1.93	4.44E-03	1.93	4.43E-03	1.93
		80	1.13E-03	1.98	1.12E-03	1.98	1.12E-03	1.99
		160	2.82E-04	2.00	2.81E-04	2.00	2.77E-04	2.01
	P^2	20	2.09E-04	-	2.09E-04	-	2.09E-04	-
		40	2.59E-05	3.01	2.59E-05	3.01	2.60E-05	3.01
		80	3.24E-06	3.00	3.24E-06	3.00	3.25E-06	3.00
		160	4.04E-07	3.00	4.05E-07	3.00	4.07E-07	3.00
B	P^1	20	4.01E-03	-	2.93E-03	-	2.68E-03	-
		40	9.94E-04	2.01	7.24E-04	2.02	6.62E-04	2.01
		80	2.47E-04	2.00	1.80E-04	2.00	1.65E-04	2.00
		160	6.17E-05	2.00	4.51E-05	2.00	4.13E-05	2.00
	P^2	20	1.02E-04	-	1.65E-04	-	2.27E-04	-
		40	1.27E-05	3.01	2.09E-05	2.98	2.99E-05	2.92
		80	1.58E-06	3.00	2.61E-06	3.00	3.76E-06	2.99
		160	1.97E-07	3.00	3.26E-07	3.00	4.68E-07	3.00
C	P^1	20	3.95E-03	-	2.91E-03	-	2.67E-03	-
		40	9.86E-04	2.00	7.22E-04	2.02	6.62E-04	2.01
		80	2.46E-04	2.00	1.80E-04	2.00	1.65E-04	2.00
		160	6.16E-05	2.00	4.50E-05	2.00	4.12E-05	2.00
	P^2	20	1.01E-04	-	1.59E-04	-	2.13E-04	-
		40	1.26E-05	3.00	2.05E-05	2.95	2.89E-05	2.88
		80	1.57E-06	3.00	2.59E-06	2.99	3.69E-06	2.97
		160	1.97E-07	3.00	3.24E-07	3.00	4.64E-07	2.99

(b) nonuniform meshes

			$\gamma = 1.0$		$\gamma = 1.5$		$\gamma = 2.0$	
		N	error	order	error	order	error	order
A	P^1	20	1.72E-02	-	1.71E-02	-	1.71E-02	-
		40	4.56E-03	1.91	4.55E-03	1.91	4.54E-03	1.91
		80	1.14E-03	2.00	1.14E-03	2.00	1.13E-03	2.00
		160	2.86E-04	2.00	2.84E-04	2.00	2.81E-04	2.01
	P^2	20	2.36E-04	-	2.36E-04	-	2.36E-04	-
		40	2.85E-05	3.05	2.85E-05	3.05	2.85E-05	3.05
		80	3.61E-06	2.98	3.61E-06	2.98	3.61E-06	2.98
		160	4.50E-07	3.00	4.51E-07	3.00	4.51E-07	3.00
B	P^1	20	4.14E-03	-	3.11E-03	-	2.93E-03	-
		40	1.04E-03	2.00	7.80E-04	2.00	7.30E-04	2.01
		80	2.54E-04	2.03	1.91E-04	2.03	1.80E-04	2.02
		160	6.32E-05	2.01	4.75E-05	2.00	4.47E-05	2.01
	P^2	20	1.08E-04	-	1.70E-04	-	2.31E-04	-
		40	1.32E-05	3.03	2.14E-05	2.99	3.03E-05	2.93
		80	1.67E-06	2.98	2.70E-06	2.98	3.85E-06	2.98
		160	2.09E-07	3.00	3.37E-07	3.00	4.81E-07	3.00
C	P^1	20	3.98E-03	-	3.04E-03	-	2.87E-03	-
		40	1.01E-03	1.98	7.60E-04	2.02	7.12E-04	2.01
		80	2.54E-04	2.00	1.91E-04	1.99	1.79E-04	1.99
		160	6.34E-05	2.00	4.76E-05	2.00	4.47E-05	2.00
	P^2	20	1.10E-04	-	1.69E-04	-	2.26E-04	-
		40	1.35E-05	3.02	2.13E-05	2.99	2.97E-05	2.92
		80	1.66E-06	3.03	2.66E-06	3.00	3.77E-06	2.98
		160	2.07E-07	3.00	3.33E-07	3.00	4.74E-07	2.99

TABLE 5.3. L^2-norm errors and convergence orders for LDG method with different parameter combinations in one-dimensional space. $\theta = 0.75$.

		uniform mesh		nonuniform mesh	
	N	error	order	error	order
P^0	20	1.86E-01	-	1.96E-01	-
	40	8.86E-02	1.07	9.05E-02	1.11
	80	4.46E-02	0.99	4.60E-02	0.98
	160	2.26E-02	0.98	2.32E-02	0.99
P^1	20	3.05E-02	-	3.29E-02	-
	40	9.03E-03	1.75	9.28E-03	1.83
	80	2.42E-03	1.90	2.45E-03	1.92
	160	6.17E-04	1.97	6.28E-04	1.96
P^2	20	1.51E-03	-	1.49E-03	-
	40	2.05E-04	2.88	1.89E-04	2.98
	80	3.39E-05	3.10	2.63E-05	2.85
	160	3.91E-06	2.61	3.73E-06	2.82
P^3	20	2.61E-04	-	3.49E-04	-
	40	4.56E-05	2.52	3.57E-05	3.29
	80	7.58E-06	2.59	1.13E-05	1.66
	160	2.30E-06	1.72	2.54E-06	2.15

TABLE 5.4. L^2-norm errors and convergence orders on uniform and nonuniform meshes. Exact solution $[\sin(x-t)]^{2.6}$ and $c=d=1$.

We will also want to extend the work of [9] and consider the local estimate when the problem is convection-dominated and equipped with the Dirichlet boundary condition such that the boundary layer exists. Moreover, the fully-discrete LDG method with suitable time-marching algorithms will be considered.

APPENDIX A. PROOF OF THE IDENTITY (3.40)

Now we supplement the proof of (3.40), by noticing the following simple property: if the considered function depends solely on one single variable, the two-dimensional generalized Gauss–Radau projection P_{θ_1,θ_2} reduces to one-dimensional generalized Gauss–Radau projection, at a certain direction.

For example, assume $z_K(x,y)=z_K(x)$ be any function depending solely on x. Then it follows from (3.13) that $(P_{\theta_1,\theta_2}z_K)(x,y)=P^x_{\theta_1}z_K(x)$ and thus there holds

$$\int_{I_i}\eta_{z_K}v_h\mathrm{d}x=0,\quad \forall v_h\in P^{k-1}(I_i);\qquad (\eta_{z_K})^{(\theta_1)}_{i+\frac{1}{2}}=0,$$

for any $i=1,2,\ldots,N$, where $\eta_{z_K}=z_K-P_{\theta_1,\theta_2}z_K$ depends solely on x. This will lead directly to

$$\begin{aligned}H^{1,\theta_1}_{ij}(\eta_{z_K},v_h)=&\int_{I_i}\Big[\eta_{z_K}\int_{J_j}\frac{\partial v_h}{\partial x}\mathrm{d}y\Big]\mathrm{d}x-(\eta_{z_K})^{(\theta_1)}_{i+\frac{1}{2}}\int_{J_j}(v_h^-)_{i+\frac{1}{2},y}\mathrm{d}y\\&+(\eta_{z_K})^{(\theta_1)}_{i-\frac{1}{2}}\int_{J_j}(v_h^+)_{i-\frac{1}{2},y}\mathrm{d}y=0,\end{aligned}\tag{A.1}$$

where we have used the simple fact that $\int_{J_j}\frac{\partial v_h}{\partial x}\mathrm{d}y\in P^{k-1}(I_i)$.

On the other hand, assume $z_K(x,y)=z_K(y)$ be any function depending solely on y. Then we have $(P_{\theta_1,\theta_2}z_K)(x,y)=P^y_{\theta_2}z_K(y)$ and $\eta_{z_K}=z_K-P_{\theta_1,\theta_2}z_K$ depends

solely on y. Hence we have

$$\frac{\partial \eta_{z_K}}{\partial x} = 0, \quad [\![\eta_{z_K}]\!]_{i\pm\frac{1}{2},y} = 0.$$

A simple integration by parts yields

$$\begin{aligned} H_{ij}^{1,\theta_1}(\eta_{z_K}, v_h) = &- \int_{K_{ij}} \frac{\partial \eta_{z_K}}{\partial x} v_h \mathrm{d}x\mathrm{d}y - \widetilde{\theta}_1 \int_{J_j} \left([\![\eta_{z_K}]\!] v_h^- \right)_{i+\frac{1}{2},y} \mathrm{d}y \\ &- \theta_1 \int_{J_j} \left([\![\eta_{z_K}]\!] v_h^+ \right)_{i-\frac{1}{2},y} \mathrm{d}y = 0. \end{aligned} \tag{A.2}$$

Now we come back to prove (3.40). For any $z \in P^{k+1}(\Omega_h)$, define

$$z_K = z \cdot \mathbb{1}_K, \tag{A.3}$$

where $\mathbb{1}_K$ is the characteristic function, which is equal to one on the element K and zero otherwise. This implies the decomposition $z = \sum_{K\in\Omega_h} z_K$. Since $H_{ij}^{1,\theta_1}(\cdot,\cdot)$ is a bilinear functional, we just need to prove for any $K \in \Omega_h$ that

$$H_{ij}^{1,\theta_1}\left(\eta_{z_K}, v_h\right) = 0, \qquad \forall v_h \in Q^k(K_{ij}). \tag{A.4}$$

Noticing the definition of generalized Gauss–Radau projection P_{θ_1,θ_2}, it is easy to see that (A.4) holds for any $z_K \in Q^k(K)$. Thus we only need to verify (A.4) for both $z_K(x,y) = x^{k+1}\mathbb{1}_K$ and $z_K(x,y) = y^{k+1}\mathbb{1}_K$. Since both can be looked upon as the single-variable function, (A.4) holds obviously, due to (A.1) and (A.2). Now the proof is finished. □

References

1. F. Bassi, S. Rebay, *A high-order accurate discontinuous finite element method for the numerical solution of the compressible Navier-Stokes equations*, J. Comput. Phys., 131 (1997), pp. 267–279.
2. J. L. Bona, H. Chen, O. Karakashian, and Y. Xing, *Conservative, discontinuous-Galerkin Methods for the generalized Korteweg–de Vries equation*, Math. Comp., 82 (2013), pp. 1401–1432.
3. S. C. Brenner, L. R. Scott, The mathematical theory of finite element methods, Springer-Verlag, 1998.
4. P. Castillo, *An optimal error estimate for the local discontinuous Galerkin method*, Discontinuous Galerkin methods: Theory, Computation and Applications (B. Cockburn, G. E. Karniadakis, and C. W. Shu, eds), Lectures Notes in Computational Science and Engineering, vol. 11, Springer-Verlag, 2000, pp. 285–290.
5. P. Castillo, B. Cockburn, I. Perugia, and D. Schötzau, *An a priori error analysis of the local discontinuous Galerkin method for elliptic problems*, SIAM. J. Numer. Anal., 38 (2000), pp. 1676–1706.
6. P. Castillo, B. Cockburn, D. Schötzau and C. Schwab, *Optimal a priori error estimates for the hp-version of the local discontinuous Galerkin method for convection-diffusion problems*, Math. Comp., 71 (2001), pp. 455–478.
7. Y. Cheng and C.-W. Shu, *A discontinuous finite element method for time dependent partial differential equations with higher order derivatives*, Math. Comp., 77 (2008), pp. 699–730.
8. Y. Cheng and C.-W. Shu, *Superconvergence of discontinuous Galerkin and local discontinuous Galerkin schemes for linear hyperbolic and convection-diffusion equations in one space dimension*, SIAM. J. Numer. Anal., 47 (2010), pp. 4044–4072.
9. Y. Cheng, F. Zhang, and Q. Zhang, *Local analysis of local discontinuous Galerkin method for the time-dependent singularity perturbed problem*, J. Sci. Comput., 63 (2015), pp. 452–477.
10. B. Cockburn, G. Kanschat, I. Perugia and D. Schötzau, *Superconvergence of the local discontinuous Galerkin method for elliptic problems on Cartesian grids*, SIAM. J. Numer. Anal., 39 (2001), pp. 264–285.

11. B. Cockburn and C.-W. Shu, *TVB Runge-Kutta local projection discontinuous Galerkin finite element method for conservation laws II: General framework*, Math. Comp., 52 (1989), pp. 411–435.
12. B. Cockburn and C.-W. Shu, *The Runge-Kutta discontinuous Galerkin method for conservation laws V: Multidimensional systems*, J. Comput. Phys., 141 (1998), pp. 199–224.
13. B. Cockburn and C.-W. Shu, *The local discontinuous Galerkin method for time-dependent convection-diffusion systems*, SIAM. J. Numer. Anal., 35 (1998), pp. 2440–2463.
14. B. Cockburn and C.-W. Shu, *Runge-Kutta discontinuous Galerkin methods for convection-dominated problems*, J. Sci. Comput., 16 (2001), pp. 173–261.
15. D. A. Di Pietro and A. Ern, Mathematical aspects of discontinuous Galerkin methods, Springer, New York, 2012.
16. G. H. Golub and C. F. Van Loan, Matrix Computations, Posts and Telecom Press, 2011.
17. S. Gottlieb, C.-W. Shu and E. Tadmor, *Strong stability preserving high order time discretization methods*, SIAM Rev., 43 (2001), pp. 89–112.
18. J. S. Hesthaven and T. Warburton, Nodal discontinuous Galerkin methods: algorithms, analysis, and applications, Springer, New York, 2008.
19. H. Liu and N. Polymaklam, *A local discontinuous Galerkin method for the Burgers-Poisson equation*, Numer. Math., 129 (2015), pp. 321–351.
20. X. Meng, C.-W. Shu, and B. Wu, *Optimal error estimates for discontinuous Galerkin methods based on upwind-biased fluxes for linear hyperbolic equations*, to appear in Math. Comp.
21. W. H. Reed, and T. R. Hill, *Triangular mesh method for the neutron transport equation*, Technical report LA-UR-73-479, Los Alamos Scientific Laboratory, Los Alamos, NM, 1973.
22. B. Rivière, Discontinuous Galerkin methods for solving elliptic and parabolic equations: theory and implementation, Society for Industrial and Applied Mathematics, 2008.
23. C.-W. Shu, *Discontinuous Galerkin methods: general approach and stability, Numerical Solutions of Partial Differential Equations*, S. Bertoluzza, S. Falletta, G. Russo and C.-W. Shu, in *Advanced Courses in Mathematics CRM Barcelona*, 149-201. Birkhäuser, Basel, 2009.

Department of Mathematics, Nanjing University, Nanjing 210093, Jiangsu Province, China

E-mail address: ycheng@smail.nju.edu.cn

Department of Mathematics, Harbin Institute of Technology, Harbin 150001, Heilongjiang Province, China

E-mail address: xiongmeng@hit.edu.cn

Department of Mathematics, Nanjing University, Nanjing 210093, Jiangsu Province, China

E-mail address: qzh@nju.edu.cn